LC GC europe
solutions for separation scientists

June 2018
Volume 31 Number 6
www.chromatographyonline.com

The **most advanced** nitrogen generator on the market today

- **Productivity**
  Built to exacting standards in our high-tech UK manufacturing facility, Genius XE gives you 24/7 365 nitrogen on-demand.
- **Confidence**
  Latest generation technology gives you greater confidence in analytical accuracy and the peace of mind of having a global leader in your lab.
- **Convenience**
  Smaller, more discrete, and easier to use than ever before thanks to PeakOS™, Genius XE is the ultimate solution for zero-stress nitrogen gas in the lab.
- **Versatility**
  With flexible flow rates and purity up to 99.5%, Genius XE is a versatile solution for various instrument gas needs including LC-MS, ELSD or sample evaporators.

Genius **XE 70** Genius **XE 35**

Contact us today to discover more!

Web: www.peakscientific.com/genius **Email:** discover@peakscientific.com

LC GC
europe
solutions for separation scientists

June 2018
Volume 31 Number 6
www.chromatographyonline.com

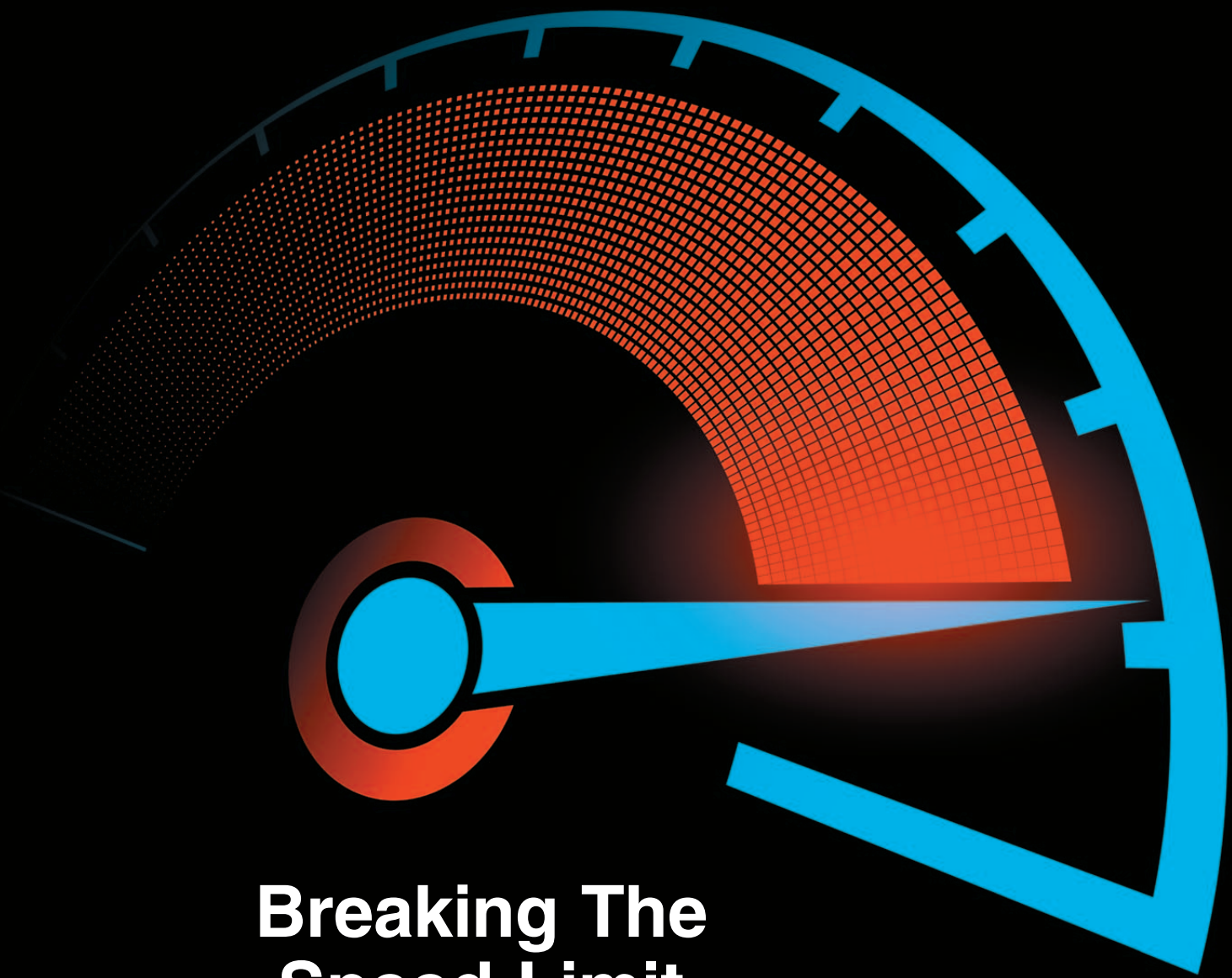

Breaking The Speed Limit

Advances in ultrafast chiral chromatography

UBM

LC TROUBLESHOOTING
Peak purity in LC

BIOPHARMACEUTICAL PERSPECTIVES
Top-to-bottom HPLC–MS methods

PERSPECTIVES IN MODERN HPLC
Characterizing antibody–drug conjugates

HUMAN HEALTH

ENVIRONMENTAL HEALTH

WHOSE TRIPLE QUAD CAN GIVE YOU 15% MORE TIME?

SIMPLE: PERKINELMER.

Whether you're performing environmental, food, or industrial testing, your lab needs to analyze more and increasingly complex samples under tighter regulatory standards. Because our new QSight™ triple-quad LC/MS/MS needs no routine cleaning and maintenance, you get up to 15% more uptime (that's up to *35 more days per year*) to take on your increased testing workload. Plus, our patented technology delivers exceptional sensitivity and reliability along with all that productivity.

QSight: A triple quad that simply knows the value of time.

Learn more at www.perkinelmer.com/QSight

PerkinElmer®
For the Better

"So you're sure this protein has a molecular weight of 150,000?"
"According to our assumptions, that's correct."

That's the problem with relying on the assumptions of column calibration to characterize macromolecules. You don't really know if your standards and your samples are the same! Perhaps that's why every major pharmaceutical and biotechnology company, as well as most federal regulatory agencies are switching from relative methods to Wyatt Technology's absolute measurements. We'll show you how to end your dependence on reference standards, in order to make you and your products a whole lot more convincing. See our webinar on Absolute Biophysical Characterization at wyatt.com/Absolute.

WYATT TECHNOLOGY
wyatt.com

June | 2018

Volume 31 Number 6

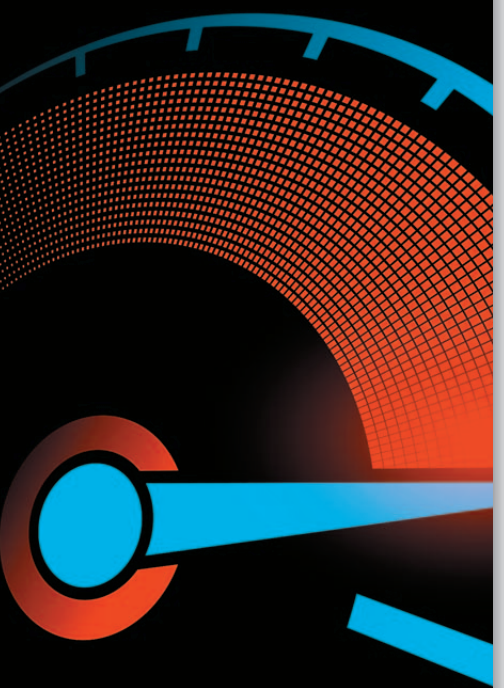

LC|GC europe
solutions for separation scientists

Cover:
Original materials courtesy:Trifonenkolvan/Shutterstock.com

COVER STORY

Features

Columns

Departments

Not Zen

Mucho Zen

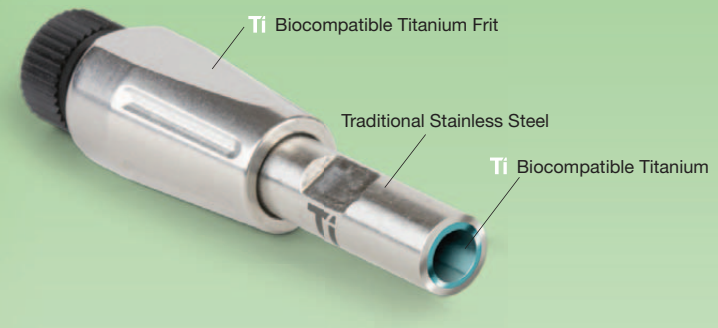

bioZen Biocompatible LC Columns for:

- Peptide Mapping
- Aggregate Analysis
- Glycan Analysis
- Peptide Quantitation
- Drug Antibody Ratio
- Intact Mass
- Intact and Fragment Analysis

Overlaid Successive Injections – Protein Priming Comparison

bioZen Titanium BioTi™ Hardware

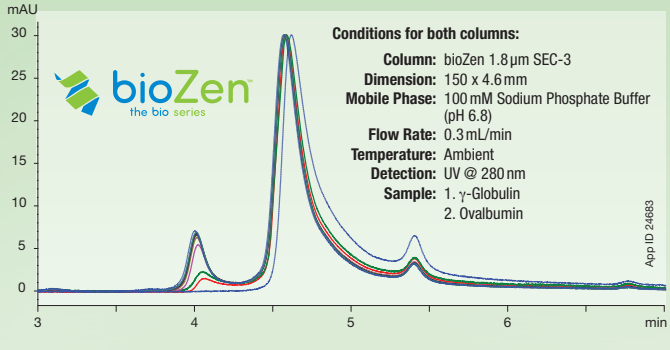

Traditional Stainless Steel

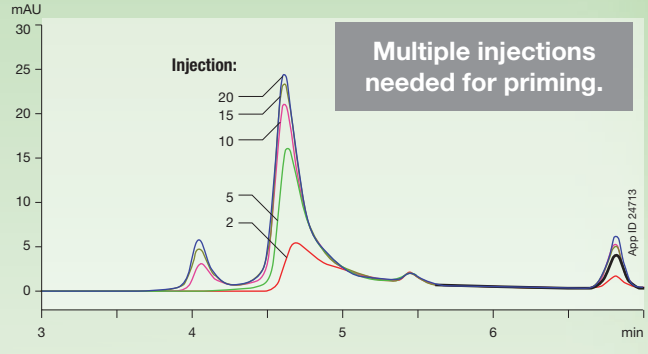

PAS9530318_W_1

phenomenex®
. . . breaking with tradition℠

www.phenomenex.com/muchozen

LC GC europe
solutions for separation scientists

Published by
UBM Americas

Subscriber Customer Service
Visit (chromatographyonline.com) to request or change a subscription or call our customer service department on +001 218 740 6877

Hinderton Point,
Lloyd Drive,
Cheshire Oaks,
Cheshire,
CH65 9HQ, UK
Tel. +44 (0)151 353 3500
Fax +44 (0)151 353 3601

Subscribe on-line at www.chromatographyonline.com

SUBSCRIPTIONS: LC•GC Europe is free to qualified readers in Europe.
To apply for a free subscription, or to change your name or address, go to www.chromatographyonline.com, click on Subscribe, and follow the prompts.
To cancel your subscription or to order back issues, please email your request to fulfill@hcl.com, putting LCE in the subject line.
Please quote your subscription number if you have it.
MANUSCRIPTS: For manuscript preparation guidelines, visit www.chromatographyonline.com or call the Editor, +44 (0)151 353 3500. All submissions will be handled with reasonable care, but the publisher assumes no responsibility for safety of artwork, photographs or manuscripts. Every precaution is taken to ensure accuracy, but the publisher cannot accept responsibility for the accuracy of information supplied herein or for any opinion expressed.
DIRECT MAIL LIST: Telephone: +44 (0)151 353 3500.
Reprints: Reprints of all articles in this issue and past issues of this publication are available (250 minimum). Contact Brian Kolb at Wright's Media, 2407 Timberloch Place, The Woodlands, TX 77380. Telephone: 877-652-5295 ext. 121. Email: bkolb@wrightsmedia.com.

LCGC Europe provides troubleshooting information and application solutions on all aspects of separation science so that laboratory-based analytical chemists can enhance their practical knowledge to gain competitive advantage. Our scientific quality and commercial objectivity provide readers with the tools necessary to deal with real-world analysis issues, thereby increasing their efficiency, productivity and value to their employer.

UCT

Push-Thru Glyphosate Purification Cartridge

Remove unwanted matrix that can lead to significant suppression and loss of ionization with glyphosate and glufosinate.

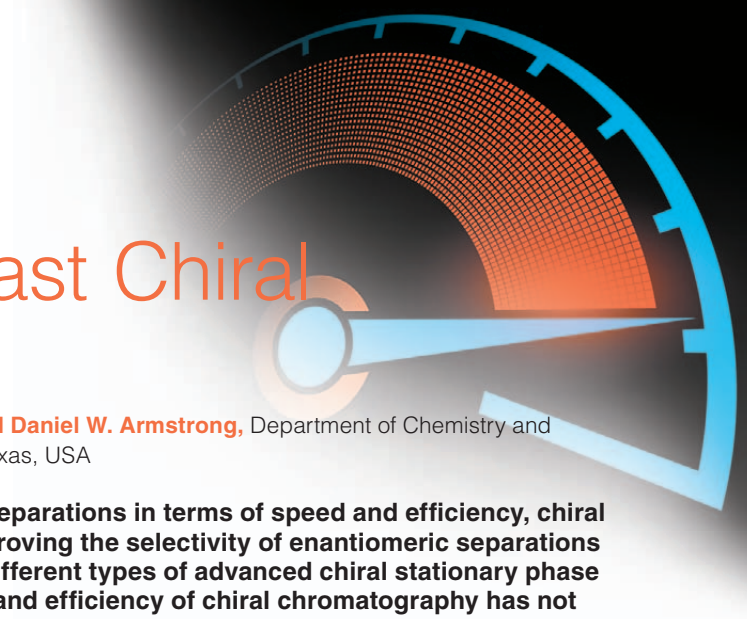

Frontiers in Ultrafast Chiral Chromatography

Daipayan Roy, Choyce A. Weatherly, M. Farooq Wahab, and Daniel W. Armstrong, Department of Chemistry and Biochemistry, The University of Texas at Arlington, Arlington, Texas, USA

Compared to the progress made in reversed phase separations in terms of speed and efficiency, chiral chromatographers have traditionally focused on improving the selectivity of enantiomeric separations by synthetic procedures. As a result, more than 50 different types of advanced chiral stationary phase chemistries are available today. Traditionally, speed and efficiency of chiral chromatography has not received attention until recently. With the availability of superficially porous particles and sub-2-µm particles, sub-minute enantiomeric separations have been achieved with the help of improved particle technology with narrow size distribution, and systematic studies on packing columns. This article covers advances made in the field of ultrafast chiral chromatography in the last decade. The development of instrumentation technology has also contributed immensely to making sub-second chiral separations a reality. Enantiomeric separations can now compete with the speed of sensors. Future directions and unanswered questions in the field of ultrafast enantiomeric separations are highlighted.

Ultrafast chiral chromatography optimization aspires to have a resolution (R_s) of 1.5 between a pair of enantiomers in the shortest possible time. Advances in stationary phases and instrument technology have changed the magnitude of the shortest possible time from nearly an hour to under a second. In the 1960s, most separations were commonly performed within the time frame of an hour (1). However, around this time, some researchers were reducing analysis times in achiral liquid chromatography (LC) by increasing the flow rate, using shorter columns packed with smaller particles, and using narrow diameter columns to increase the linear velocity (2). In high performance liquid chromatography (HPLC), a separation of three components under three minutes was achieved on silica gel in the normal-phase mode as early as 1971 (2). In gas chromatography (GC), a sub-minute separation of five components was performed with open capillaries in the late 1980s (3). Though sub-minute separations using supercritical fluid chromatography (SFC) were known to chiral chromatographers since the early 1990s (4), ultrafast separation of enantiomers using LC is currently considered one of the most challenging types of separation. (5).

Chromatographic theory indicates that the resolving power of any column depends on selectivity, efficiency, and retention factor. Decades of research involving new chiral selectors produced columns with large selectivities (α) such as cellulose or amylose derivatives, macrocyclic glycopeptides, cyclodextrins, cyclofructans, and π-complex phases on 5-µm particle silica supports. Historically, most enantiomeric separations had poor plate counts, for example, 40,000 plates/m in 25-cm long columns. This has changed in recent times and enantiomeric separation efficiencies are now approaching achiral separation efficiencies. The sudden impetus for ultrafast chiral chromatography is a result of multiple advances. The use of superficially porous particles (SPPs) and sub-2-µm fully porous particles (FPPs) is an important factor in bringing chiral separation efficiencies on par with C18 columns. In addition, state-of-the-art column packing methods has led to a rise in efficiency for enantiomeric separations from 50,000 plates/m to 250,000–300,000 plates/m (6,7). The instrumental advances have significantly contributed to ultrafast chiral chromatography as well, particularly in terms of reducing extracolumn dispersion, higher flow rates, and better detectors. Figure 1 illustrates how enantiomeric separations have evolved over the years with respect to analysis time from 5–30 min to sub-minute analyses (8). This article will discuss the breakthroughs in ultrafast enantiomeric separations and will conclude with the latest developments in the field that have managed to achieve separations in the sub-second domain.

The Particle Debate in Ultrafast Chiral Chromatography

As chiral stationary phase supports, fully porous particles (FPPs) and superficially porous particles (SPPs) have been debated in the literature as chromatographers have tried to single out a particle morphology best suited for ultrafast separations (6,7). As is evident from the van Deemter

KEY POINTS

- The latest advances in ultrafast chiral chromatography in the last decade are described.
- The debate whether superficially porous particles are better than fully porous particles is not over.
- Theoretical aspects and instrumental variables are discussed.
- The journey from sub-minute to sub-second enantiomeric separations is highlighted.

Photo Credit: Trifonenkolvan/Shutterstock.com

THE POWER OF META
NOW IN SUB-2 MICRON

FIG. 1: CHLORO

FIG. 2: METHYL

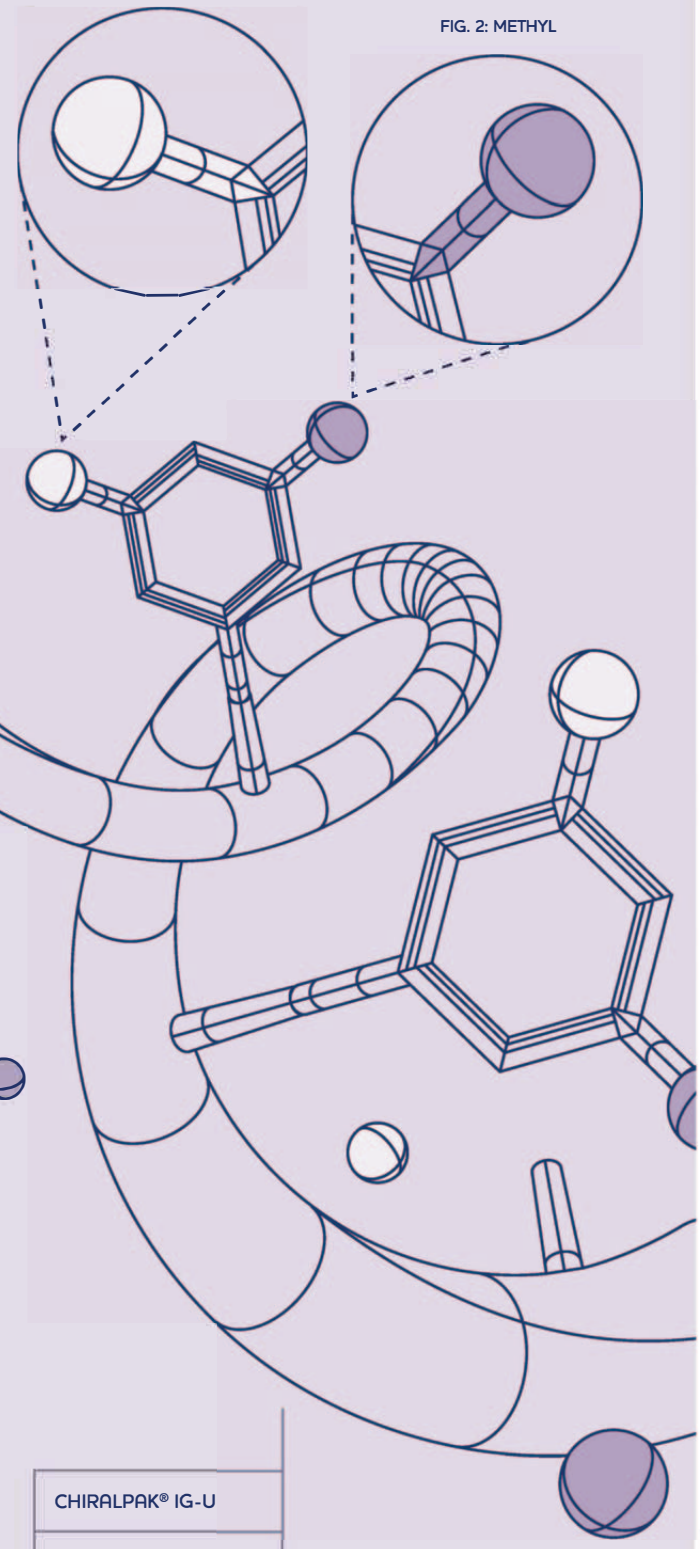

CHIRALPAK® IG-U

meta-substituted phenyl carbamate (chloro, methyl) derivative of amylose

CHIRAL CHROMATOGRAPHY **AT ULTRAFAST SPEED.**

Daicel's premier META immobilized column screening set is now available in sub-2 micron particle size.

The **CHIRALPAK® IA-U, IB-U, IC-U & IG-U** screening set offers:

- ULTRAFAST SEPARATIONS
- HIGHER RESOLUTION POWER
- SOLUTIONS IN SECONDS

Designed for use in UHPLC and optimized SFC systems.

THE POWER OF META
ULTRAFAST ANALYSIS TO MEET THE NEEDS FOR TODAY AND BEYOND

Daicel and Chiral Technologies – the Chiral Chromatography Experts.
Contact us today.

WWW.CHIRALTECH.COM

DAICEL

CHIRAL TECHNOLOGIES
DAICEL GROUP

Figure 1: Historical evolution of speeds for chromatographic separation of the enantiomers of lansoprazole, flurbiprofen, and warfarin. Adapted with permission from reference 8.

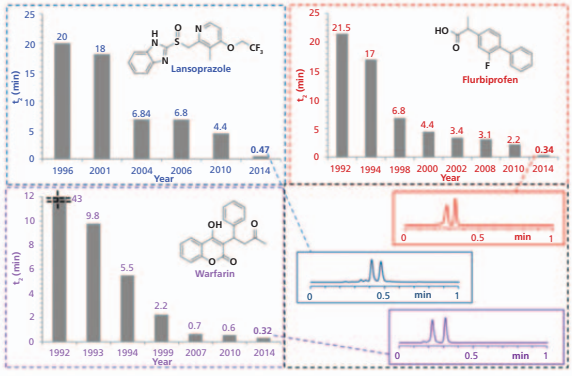

Figure 2: Ultrafast resolution in polar organic mode (POM) of the enantiomers of naproxen on the UHPLC 50 mm × 4.6 mm, 1.7-µm (R,R)-Whelk-O1 column at flow rates (mobile phase: MeCN + 0.2% AcOH + 0.07% DEA (*v/v/v*), UV detection at 254 nm, T_{col} = 25 °C). Adapted with permission from reference 6.

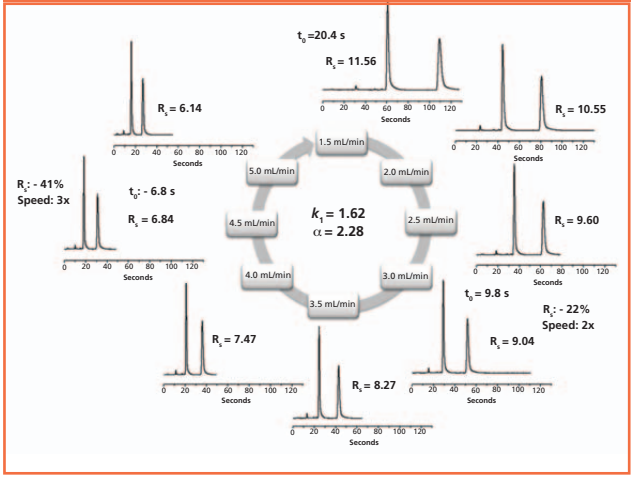

equation, smaller particles can offer lower theoretical plate heights (9),

$$H = 2\lambda\, dp + \frac{2\gamma\, Dm}{u} + \frac{\omega\, d_p^2 u}{Dm} + \frac{R\, d_f^2 u}{Ds} \qquad [1]$$

where d_p = particle diameter, H = height equivalent to a theoretical plate, D_s = diffusion coefficient of the stationary phase, d_f = film thickness, d_c = capillary diameter, D_m = diffusion coefficient of the mobile phase, λ = particle shape, and γ, ω, and R are constants. Though all the terms in the equation contribute to the broadening of an analyte band, attention to the particle size term in the equation is made herein. Smaller particles result in a lower contribution to band broadening from mass transfer along with a significant decrease in eddy dispersion. The decrease in particle size appears to be the obvious way forwards for chiral chromatographic columns, but the resulting increase in column backpressure somewhat mitigates the advantages of smaller particles.

The high efficiencies of the sub-2-µm particles are of paramount importance when performing ultrafast chiral chromatography. However, a paradigm shift in particle technology was not possible without overcoming certain hurdles. First, during the synthesis of the stationary phase, smaller particles tend to aggregate more readily than larger particles. Aggregation of smaller particles in poorly dispersive solvents can result in low and nonreproducible surface-bonded chemistry (10). Furthermore, column permeability decreases with the reduction in particle diameter as described by the Kozeny-Carman relation, which shows that permeability is inversely proportional to $(d_p)^2$ (11). For example, an approximate ninefold increase in backpressure occurs when the particle size is decreased from 5 µm to 1.7 µm. Large particle size distribution also creates problems. Tremendous advancements in the field of ultrahigh-pressure liquid chromatography (UHPLC) instrumentation have made the use of these smaller particles possible for enantiomeric separations.

Fully Porous Particle Chiral Stationary Phases

Gasparrini and co-workers were the first to bond a chiral selector to sub-2-µm FPP particles to perform ultrafast enantiomeric separations (6,12). Upon theoretical investigation, their van Deemter plots revealed a flat C-term profile up to 14 mm/s. High efficiencies were observed at higher-than-optimal flow rates as encountered in routine HPLC. A wide array of ultrafast chiral separations were shown. Gasparrini and co-workers described the process of transitioning from conventional 5-µm particle-based enantiomeric separations to sub-2-µm particle-based enantiomeric separations with UHPLC. The intrinsic kinetic performances of sub-2-µm silica were retained after bonding the chiral selector to the particles. An ultrafast separation using sub-2-µm particles at multiple flow rates is shown in Figure 2.

In the 1970s, the efficiencies of large particle-based columns were stated to remain unaffected by the size distribution of the particles as long as the deviation was lower than 40% (13). In contrast, Desmet and co-workers recently reported a linear dependence of reduced plate heights with narrow particle size distribution (14). In agreement with Desmet, Catani *et al.* showed experimentally higher efficiencies for columns packed with narrow size distribution particles compared to polydisperse particles (15). The first narrow size distribution particles were 1.9-µm FPPs. Size distribution for these particles has a standard deviation as low as 6% (16). Barhate *et al.* bonded macrocyclic glycopeptides (teicoplanin, vancomycin, and teicoplanin aglycone) to narrow size distribution silica particles (16). They reported efficiencies up to 210,000 plates/m. Lower reduced plate heights were reported with columns packed with narrow size distribution particles compared to polydispersed 1.7-µm particles. Different classes of chiral compounds, namely chiral heterocycles, amino acids, β-blockers, and pharmaceutically important drugs, were enantiomerically separated with UHPLC and SFC. Ismail *et al.* reported similar

observation with the narrow size distribution silica particles and used them for ultrafast separations (17). A problem with these small particles is the resulting frictional heating, which had been predicted four decades ago by Halász in his classical paper "*Ultimate Limits in High-Performance Liquid Chromatography*" (13) and will be discussed in a later section.

Superficially Porous Particles Bonded Chiral Stationary Phase

As pointed out earlier, sub-2-µm particles generate higher backpressures as a result of reduced column permeability. Such particles cannot be used in common HPLC systems because of limitations regarding the pressure that can be tolerated. Specially designed pumps for UHPLC systems are required. Hence the search for a particle morphology that can provide efficiencies comparable to that of sub-2-µm fully porous particles but with lower backpressures led to the advent and use of 2.7-µm SPPs for chromatographic columns. SPPs or core–shell silica particles are chromatographic supports that possess a solid, impenetrable core. This particle morphology has been applied to achiral columns and has led to high efficiencies (reduced plate heights 1.4–1.6). The SPPs exhibit much better packing homogeneity compared to FPPs (18). Better packing homogeneity across the column radius has led to a lower contribution to band broadening owing to lower eddy dispersion contributions (18). SPPs are also able to decrease other factors that contribute to band broadening, such as longitudinal diffusion and resistance to mass transfer.

Initial reports in 2012 described coated polysaccharide chiral selector on SPPs showing decreased enantiomeric selectivity compared to its fully porous counterpart (19). A reason for this observation was attributed to the reduced chiral selector loading and difficulty in reproducing coated phases on SPPs owing to their small pore size (~100–400 Å) compared to wide pore FPPS (pore sizes in the range of 1000 Å), which are used to manufacture coated chiral stationary phases.

A significant advance in the field of SPP-based chiral stationary phases occurred when bonded brush-type cyclofructan-based and macrocyclic glycopeptide chiral selectors were used. Much higher efficiencies were obtained than on FPPs while retaining or improving enantiomeric selectivity under the same mobile phase conditions (20). Another important take-away from the study pointed to the higher efficiency and significantly lower analysis times of the SPPs compared to the FPPs across different chromatographic modes, such as reversed phase, polar organic, and normal phase.

The subsequent systematic study conducted by Armstrong and co-workers highlighted the advantages of SPPs for manufacturing chiral stationary phases and performed ultrafast separations using 2.7-µm SPPs (7). The authors reported comparisons of enantiomeric separations on

Figure 3: Representative ultrafast enantiomeric separations on each of six chiral stationary phases: (a) vancomycin SPP (3 cm × 0.46 cm, 2.7-µm), MP = methanol, 4.95 mL/min, T_{col} = 60 °C, (b) teicoplanin aglycone SPP (3 cm × 0.46 cm, 2.7-µm), MP = methanol, 4.70 mL/min, T_{col} = 60 °C, (c) hydroxylpropyl-β-cyclodextrin SPP (5 cm × 0.46 cm, 2.7-µm), MP = 97:3:0.3:0.2 acetonitrile–methanol–TFA–TEA, 4.75 mL/min, T_{col} = 60 °C, (d) teicoplanin SPP (3 cm × 0.46 cm, 2.7-µm), MP = 40:60 water–methanol, 3.00 mL/min, T_{col} = 22 °C, (e) CF7-DMP SPP (3 cm × 0.46 cm, 2.7-µm), MP = 90:10 heptane–ethanol, 4.80 mL/min, T_{col} = 22 °C, (f) CF6-P SPP (10 cm × 0.46 cm, 2.7-µm), MP = 70:30:0.3:0.2 acetonitrile–methanol–TFA–TEA, 4.50 mL/min, T_{col} = 22 °C. All columns were manufactured by AZYP LLC. Adapted with permission from reference 7.

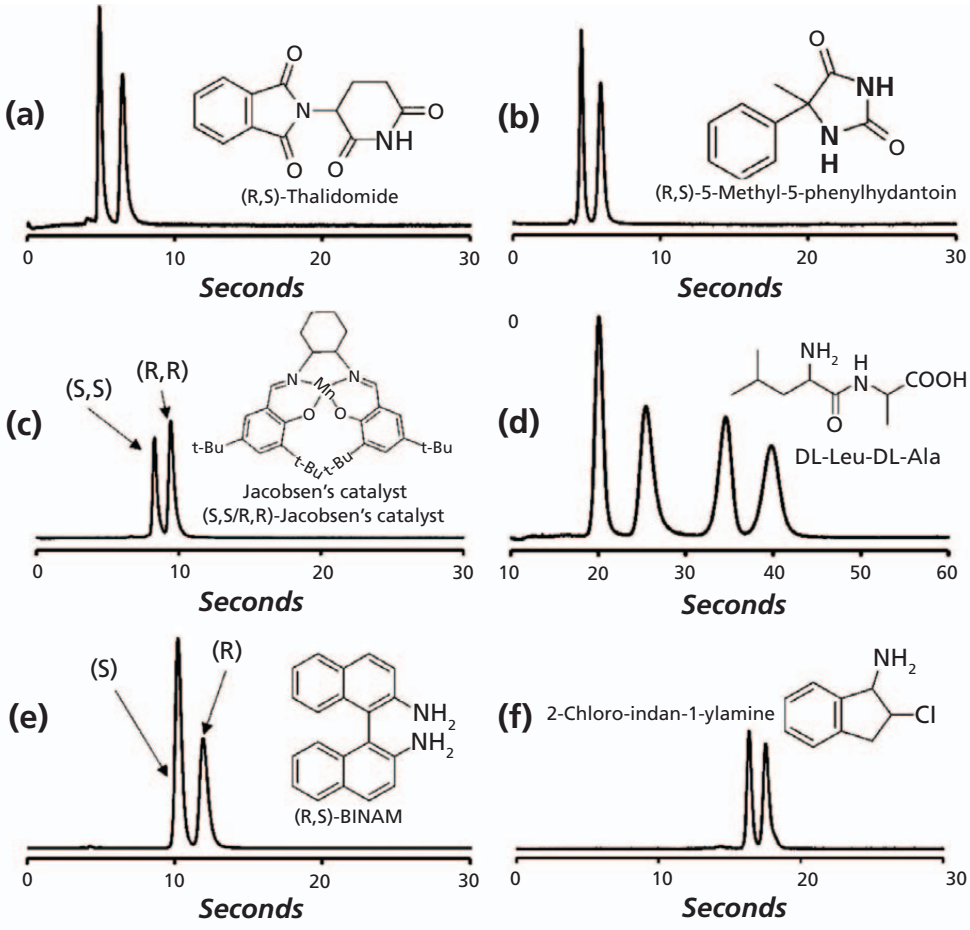

columns with multiple particle diameters and different particle morphologies ranging from 5-µm to 2.1-µm FPP and 2.7-µm SPP-based chiral stationary phases, some of them commercially obtained and some produced in-house. The superior performance of the SPPs to the commercially available chiral columns was quite apparent. Reporting reduced plate heights as low as 1.6, the group performed chiral separations for a broad range of an important class of molecules (all under a minute) using different chiral selectors, namely teicoplanin, teicoplanin aglycone, vancomycin, hydroxypropyl β-cyclodextrin, and derivatized cyclofructans (Figure 3).

The analysis time was further reduced by Wahab *et al.* who performed sub-second enantiomeric separations of multiple biologically important molecules (21). The authors successfully packed 0.5-cm columns of variable internal diameter (0.46 cm, 0.30 cm, and 0.21 cm) and reported enantiomeric separations at unprecedented speeds. Their work pointed out the necessities of multiple hardware improvements. Other reports have also pointed out the superiority of 2.7-µm SPPs over traditional 5-µm particles using geometry independent kinetic plots (22). The 5-µm particles investigated lagged both in efficiency and analysis times when compared to the 2.7-µm SPPs. The geometry independence of their results highlights the considerable impact of particle morphology on column efficiencies.

Min *et al.* tried to incorporate the advantages of both SPPs and sub-2-µm particles and synthesized 1.5-µm teicoplanin-bonded SPPs to demonstrate the potential of sub-2-µm SPPs (23). This is the only report available in this area that the authors are aware of and further studies will hopefully be conducted in the future.

Do we have an answer to the question of best particle morphology? No. A 2016 study by scientists at the University of Roma found despite the previously stated advantages of SPPs that columns with sub-2-µm FPPs outperformed the 2.7-µm SPPs; a study conducted by Ismail *et al.* highlighted the superior performance of 1.8-µm and 2.5-µm FPP

compared to the 2.6-µm SPPs. They attributed the larger surface density of the chiral selector on the SPPs as probable factor for the slower mass transfer kinetics leading to lower efficiencies (24). Recent work by the same authors using teicoplanin bonded to 2-µm SPPs has produced excellent results with efficiencies reaching 300,000 plates/m (25). This study compared the SPPs with sub-2-µm narrow size distribution silica particles and found the 2-µm SPPs to be superior in terms of efficiency and more promising towards the development of ultrafast chiral chromatography than the 1.9-µm FPPs. The findings mentioned above by independent research groups will hopefully help SPPs gain traction in the field of chiral separations. Nonetheless, particle morphology is still a hotly debated topic both from a theoretical and experimental perspective, and further research is needed to reach a consensus.

However, the major shift in particle size of the silica support from 5- to sub-2-µm has led to its adoption in multiple applications, such as ultrafast and two dimensional chromatography. The commercial availability of these columns has also helped smaller particles gain popularity. Both FPPs and SPPs have recently been used to perform multiple separations in two-dimensional liquid chromatography (2D-LC), and the promising results are sure to pave the way for further development in this field. In the past, enantiomeric separations were rarely performed in the second dimension of 2D-LC because of the slower mass transfer kinetics and problems with peak wrap-around, but recent advances in speed have allowed for the use of such chiral stationary phases in the second dimension (26).

Frictional Heating Issues with Ultrafast Chromatography

Frictional heating is an inevitable consequence of high flow rates in ultrafast achiral or chiral chromatography. Frictional heating has been documented by researchers by measuring the flow averaged temperature at the column outlet with a 10 °C rise in mobile phase temperatures found (7). Though frictional heating has been found to cause distortions in peak shapes in conventional reversed phase chromatography, it can be beneficial when performing ultrafast chiral chromatography (7). It is well known that frictional heating can be broadly classified into two types: radial and axial. Scientists studying the effects of frictional heating on chiral separations found that axial temperature gradients improved peak efficiency, but radial heating was detrimental to efficiency (7). A radial temperature gradient lowers column efficiency as a result of the distortion of the laminar flow profile. From mathematical treatments of radial heating, it can be concluded that high flow rates, higher pressure drops across the column, large column radius, and poor thermal conductivity of the mobile phase increase temperature gradients in the radial direction (centre being the hottest). The final chromatographic efficiency is a net result of the two opposing mechanisms. At high flow rates in a non-thermostated system there was a significant decrease in plate height as evident from the van Deemter plot, which was attributed to higher axial heating contributions resulting in improved efficiency (7). Though thermostating may provide higher reproducibility, it is not actively employed in most of the reported research on ultrafast chromatography because it leads to higher extracolumn volumes.

Figure 4: Single heart-cutting 2D-LC method for separation of complex mixture of closely related stereoisomers from an anti-HCV therapeutic. Conditions, first dimension (achiral): column, 2.1 mm × 150 mm, 1.6-µm Cortecs (Waters), temperature, 40 °C. Detection: UV 215 nm. Flow rate: 0.220 mL/min. Mobile phase: eluent A, 0.1% H_3PO_4 in H_2O, eluent B, 80:20 acetonitrile–methanol *(v/v)*. Step gradient: 20–45% B in 7 min, 7–20 min, 90% B, 20–32 min, 20% B. Sample frequency: 80 Hz. Conditions, second dimension (chiral): column, 4.6 mm × 50 mm, 1.9-µm teicoplanin (AZYP LLC), ambient temperature. Detection: UV 215 nm. Flow rate: 1.0 mL/min. Isocratic mobile phase: 5:95 0.1% H_3PO_4 in H_2O–acetonitrile. Sampling frequency: 240 Hz. Adapted with permission from reference 26.

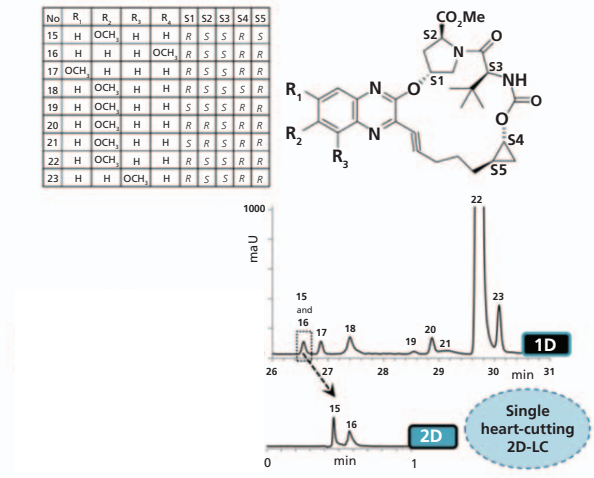

Figure 5: Ultrafast separation of oxazepam enantiomers on 2.7-µm 1 cm SPP teicoplanin column. Dependence of chromatographic signal on sampling rate and response times. The sampling rate and response times are (a) 5 Hz, 1 s. (b). 5 Hz, 0 s. (c). 250 Hz, 1 s. (d). 250 Hz, 0 s, respectively. Original work.

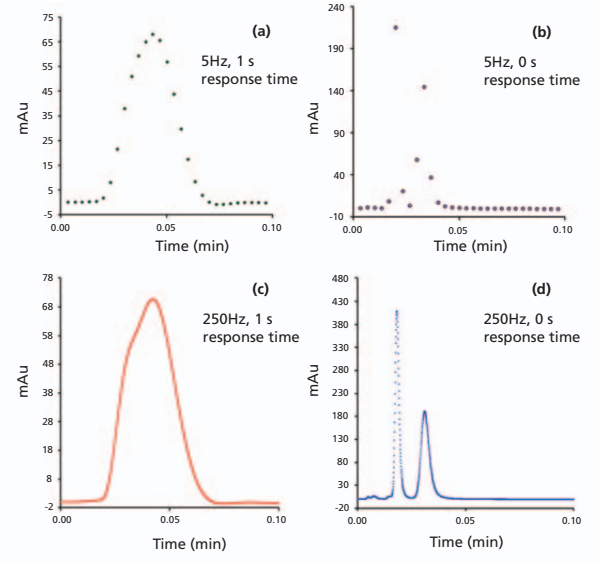

Table 1: Sampling rates and modern digital filters in chromatography instruments

Instrument	Maximum Pressure	Maximum Flow Rate	Maximum Sampling Frequency	Digital Filter Used (33)
Thermo Vanquish Horizon	150 MPa	8 mL/min at up to 50 Mpa and 5 mL/min at up to 150 Mpa	250 Hz	Savitsky-Golay, Moving Average, Olympic filter, Gaussian weighted moving average
Agilent 1290 Infinity II	130 MPa	5 mL/min	240 Hz	Gaussian weighted moving average
Waters Acquity UPLC	130 MPa	4 mL/min	80 Hz	Hamming filter
Jasco LC-4000	130 MPa	5 mL/min	100 Hz	RC filter, Centred moving average Simple moving average
Shimadzu Nexera 2	130 Mpa	5 mL/min	200 Hz	RC filter

Figure 6: Sub-second separation of oxazepam enantiomers. Conditions: Column: 1 cm × 0.3 cm, 2.7-µm SPP Teicoplanin (AZYP LLC), mobile phase: 100% methanol, flow rate: 7.5 mL/min, UV–vis detection at 254 nm. Original work.

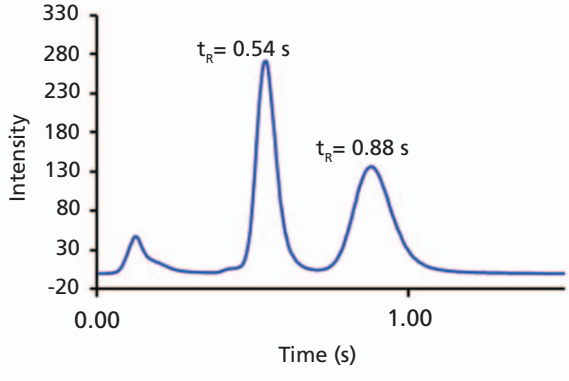

Instrumental and Practical Considerations

It is widely accepted that chromatographic instrumentation lags behind column technology. Advances in instrumentation are as important as high-efficiency columns when it comes to ultrafast chromatography. When looking particularly at fast eluting peaks, the effect of different instrumental parameters seems to be much more profound. Achieving ultrafast separations on HPLC systems is highly difficult owing to their limitation in a variety of aspects, particularly backpressure tolerance and extracolumn volumes. Chromatographers have therefore moved on to the more developed UHPLC systems introduced commercially in 2004. Commercial UHPLC systems have come a long way since then, and current systems are equipped with highly sensitive UV detectors, lower extracolumn volumes, and better electronics resulting in a better representation of a chromatographic system to the end user.

Ultrafast separations pose several instrumental challenges. These include the requirements of fast chromatographic detectors, high-pressure pumps with 8 mL/min flow rates, and most importantly, an understanding of chiral column packing technology. The downside of the small particles is a decrease in column permeability, which leads to higher backpressures and the need for more sophisticated pumps to handle higher pressures and flow rates (for example, up to 800 bar and 8 mL/min).

Researchers utilized the advances in instrumentation and reported transitioning from chiral HPLC to chiral UHPLC (6), using chiral stationary phase bonded to sub-2-µm particles to produce high backpressure. Separation was performed at flow rates up to 6 mL/min to achieve ultrafast speeds and to justify the need for UHPLC systems. Researchers at Merck also managed to develop an ultrafast screening protocol on UHPLC systems for pharmaceutically important compounds using multiple columns operating under reversed phase conditions (27). Modern-day UHPLC systems vary in the pressure that they can tolerate and flow rates up to which they can operate.

Extracolumn Band Broadening

Extracolumn band broadening stands out as a disadvantage while performing ultrafast separations. Any peak convolution process taking place outside the column including contributions to band broadening from the injector, tubing, detector volume, and detector electronics are deemed as extracolumn effects. Though decreasing contributions from detector volume and detector electronics are beyond a typical user's prerogative, band broadening can be significantly lowered by using narrow internal diameter (i.d.) tubing and using ultralow dispersion injectors now commercially available. A study showed a staggering 50% decrease in efficiency of the first eluted peak when tubing was changed from 75 µm i.d. tubing to regular blue PEEK tubing (254 µm i.d.) (28). A reader with the intention of performing ultrafast separations must therefore pay close attention to the choice of tubing to attain maximum efficiency from a given system.

Sampling Rates and Response Times

The most commonly used detector in LC is the diode array detector (DAD). Detector sampling rates and detector response times have become important aspects of ultrafast chromatography. Peak shapes, peak width, and baseline noise can vary considerably when changing detector settings. The sampling frequency can be varied in most HPLC and UHPLC systems. According to Shannon's theorem (21), to accurately capture an analytical signal the minimum sampling frequency must be twice the maximum frequency components in the signal being acquired. Performing Fourier analysis on a

chromatogram can extract the frequency components and consequently uncover the minimum sampling frequency required for analysis of the analyte signal. According to the study conducted by Wahab *et al.,* by simulating a sub-second separation current instrumentation is capable of sampling data at frequencies sufficient for commercially available high-efficiency columns, but the authors predicted that with the advent of higher efficiency columns higher sampling rates might be required to perform an accurate representation of the signal (21). The highest available sampling frequency in a UHPLC system varies across different manufacturers, some being as high as 250 Hz. This high sampling rate results in higher baseline noise and manufacturers have tried to tackle this problem by using digital filters such as "Savitzky-Golay", "Gaussian rectangular weighted moving average", "rectangular moving average", "low pass RC", and "Hamming filter" to eliminate high frequency signal components and thereby reduce baseline noise (33). These filters are often anonymous in the instrument software; however, users can see the rise time or the response times in the detector settings of the method. Response times are defined as the time it takes for a unit step-function to go from 10% to 90% of the signal. Each digital filter can uniquely distort the peak shape if the response time is not chosen judiciously. Figure 5 shows the massive impact of sampling frequency and response times on a chromatographic signal. Only with the correct choice of both parameters can the desired chromatogram be obtained.

Table 1 gives a brief overview of a range of UHPLC instruments available from a variety of manufacturers with regards to their pressure tolerance, maximum flow rate at which they can operate, maximum sampling frequency, and the digital filter they use (data obtained from manufacturer's website).

Where do we stand in terms of speed? Following optimization of both column and instrumental parameters, chiral chromatography has reached new heights unimaginable even a few years ago. As described earlier, the time limit for an "ultrafast separation" is arbitrarily chosen to be under one minute. This definition is sure to change in future, and as of now, sub-second chromatography is no longer a dream. Enantiomeric separations under a second have now been performed both with LC and SFC and it has opened avenues for a variety of applications for which chromatography was earlier considered too slow (30). Pioneering work by researchers in the United States, optimizing both instrumental and practical factors coupled with the development of packing techniques for columns as small as 0.5 cm, has led to achiral and chiral separations of a wide range of analytes under a second (21). Researchers in Italy have also reported sub-second separation using a 1-cm long pi-complex chiral selector-based column (24). Further increases in speed of chromatographic separations have recently been achieved, and as many as ten analytes have been separated under a second (29). This unforeseen speed in the domain of chromatographic separation is sure to create a huge impact in upcoming research in this area. Figure 6 illustrates

the sub-second separation of oxazepam enantiomers. Interestingly, chromatography can now be completed in a time domain that was previously imited to sensors (29).

Conclusions

The progress of enantiomeric separations, particularly with regards to speed, has been astonishing in the last few years. The dream of ultrafast chiral separation has been realized by groundbreaking work by researchers both in industry and academia. Commercial availability of sub-2-µm FPP and 2.7-µm SPP-based chiral stationary phases will further accelerate research in the domain of ultrafast chiral separations (21,29,31,32). Since most chiral stationary phases used in LC can also be used in SFC, both the techniques will benefit from these advances. Owing to the tremendous progress in this area, the need for better instrumentation seems to be imminent. Finally, as these developments result in even faster separations, the impact will be felt in a multitude of diverse fields, such as monitoring short lived intermediates and on-line reaction profiles, and even more so if the entire system can be miniaturized.

References

(1) C.G. Horvath, B. Preiss, and S.R. Lipsky, *Analytical Chemistry* **39**, 1422–1428 (1967).

(2) D. Randau and W. Schnell, *Journal of Chromatography A* **57**, 373–381(1971).

(3) Z. Liu and J.B. Phillips, *Journal of Microcolumn Separations* **1**, 249–256 (1989).

(4) F. Gasparrini, D. Misiti, and C. Villani, *TrAC Trends in Analytical Chemistry* **12**, 137–144 (1993).

(5) T.J. Ward and K.D. Ward, *Encyclopedia of Analytical Chemistry* (John Wiley & Sons, Ltd., 2000).

(6) D. Kotoni, A. Ciogli, C. Molinaro, I. D'Acquarica, J. Kocergin, T. Szczerba, H. Ritchie, C. Villani, and F. Gasparrini, *Analytical Chemistry* **84**, 6805–6813 (2012).

(7) D.C. Patel, Z.S. Breitbach, M.F. Wahab, C.L. Barhate, and D.W. Armstrong, *Analytical Chemistry* **87**, 9137–9148 (2015).

(8) E.L. Regalado and C.J. Welch, *Journal of Separation Science* **38**, 2826–2832 (2015).

(9) J.J. Van Deemter, F. Zuiderweg, and A.V. Klinkenberg, *Chemical Engineering Science* **5**, 271–289 (1956).

(10) R. Hayes, A. Ahmed, T. Edge, and H. Zhang, *Journal of Chromatography A* **1357**, 36–52 (2014).

(11) P. Carman, *Chemical Engineering Research and Design* **75**, S32–S48 (1997).

(12) G. Cancelliere, A. Ciogli, I. D'Acquarica, F. Gasparrini, J. Kocergin, D. Misiti, M. Pierini, H. Ritchie, P. Simone, and C. Villani, *Journal of Chromatography A* **1217**, 990–999 (2010).

(13) I. Halász, R. Endele, and J. Asshauer, *Journal of Chromatography A* **112**, 37–60 (1975).

(14) D. Cabooter, A. Fanigliulo, G. Bellazzi, B. Allieri, A. Rottigni, and G. Desmet, *Journal of Chromatography A* **1217**, 7074–7081 (2010).

(15) M. Catani, O.H. Ismail, A. Cavazzini, A. Ciogli, C. Villani, L. Pasti, C. Bergantin, D. Cabooter, G. Desmet, and F. Gasparrini, *Journal of Chromatography A* **1454**, 78–85 (2016).

(16) C.L. Barhate, M.F. Wahab, Z.S. Breitbach, D.S. Bell, and D.W. Armstrong, *Analytica Chimca Acta* **898**, 128–137 (2015).

(17) O.H. Ismail, A. Ciogli, C. Villani, M. De Martino, M. Pierini, A. Cavazzini, D.S. Bell, and F. Gasparrini, *Journal of Chromatography A* **1427**, 55–68 (2016).

(18) M.F. Wahab, D.C. Patel, R.M. Wimalasinghe, and D.W. Armstrong, *Analytical Chemistry* **89**, 8177–8191 (2017).

(19) K. Lomsadze, G. Jibuti, T. Farkas, and B. Chankvetadze, *Journal of Chromatography A* **1234**, 50–55 (2012).

(20) D.A. Spudeit, M.D. Dolzan, Z.S. Breitbach, W.E. Barber, G.A. Micke, and D.W. Armstrong, *Journal of Chromatography A* **1363**, 89–95 (2014).

(21) M.F. Wahab, R.M. Wimalasinghe, Y. Wang, C.L. Barhate, D.C. Patel, and D.W. Armstrong, *Analytical Chemistry* **88**, 8821–8826 (2016).

(22) D.C. Patel, Z.S. Breitbach, J. Yu, K.A. Nguyen, and D.W. Armstrong, *Analytica Chimca Acta* **963**, 164–174 (2017).

(23) Y. Min, Z. Sui, Z. Liang, L. Zhang, and Y. Zhang, *Journal of Pharmaceutical and Biomedical Analysis* **114**, 247–253 (2015).

(24) O.H. Ismail, L. Pasti, A. Ciogli, C. Villani, J. Kocergin, S. Anderson, F. Gasparrini, A. Cavazzini, and M. Catani, *Journal of Chromatography A* **1466**, 96–104 (2016).

(25) O.H. Ismail, M. Antonelli, A. Ciogli, C. Villani, A. Cavazzini, M. Catani, S. Felletti, D.S. Bell, and F. Gasparrini, *Journal of Chromatography A* **1520**, 91–102 (2017).

(26) C.L. Barhate, E.L. Regalado, N.D. Contrella, J. Lee, J. Jo, A.A. Makarov, D.W. Armstrong, and C.J. Welch, *Analytical Chemistry* **89**, 3545–3553 (2017).

(27) C.L. Barhate, L.A. Joyce, A.A. Makarov, K. Zawatzky, F. Bernardoni, W.A. Schafer, D.W. Armstrong, C.J. Welch, and E.L. Regalado, *Chemical Communications* **53**, 509–512 (2017).

(28) D.C. Patel, M.F. Wahab, D.W. Armstrong, and Z.S. Breitbach, *Journal of Chromatography A* **1467**, 2–18 (2016).

(29) D.C. Patel, M.F. Wahab, T.C. O'Haver, and D.W. Armstrong, *Analytical Chemistry* **90**, 3349–3356 (2018).

(30) A. Ciogli, O.H. Ismail, G. Mazzoccanti, C. Villani, and F. Gasparrini, *J. Sep. Sci.* **41**, 1307–1318 (2018).

(31) G. Hellinghausen, D. Roy, Y. Wang, J.T. Lee, D.A. Lopez, C.A. Weatherly, and D.W. Armstrong, *Talanta* **181**, 132–141 (2018).

(32) C.L. Barhate, D.A. Lopez, A.A. Makarov, X. Bu, W.J. Morris, A. Lekhal, R. Hartman, D.W. Armstrong, and E.L. Regalado, *Journal of Chromatography A* 1539, **87**–92 (2018).

(33) M.F. Wahab, P.K. Dasgupta, A.F. Kadjo, and D.W. Armstrong, *Analytica Chimica Acta* **907**, 31–44 (2016).

Daipayan Roy is a PhD candidate at the University of Texas at Arlington, USA. His research interests include high throughput chiral and achiral separations using HPLC, HILIC, SFC, and MS.

Choyce Weatherly is a research engineering scientist at the University of Texas at Arlington. He completed his Ph.D. at the University of Texas at Arlington. His research includes method development, data analysis, and chiral–achiral separation techniques using HPLC, HPLC–MS, GC, GC–MS, and SFC.

M. Farooq Wahab is currently a research engineering scientist at the University of Texas at Arlington. He undertook a postdoctoral fellowship with Professor Armstrong after completing his Ph.D. at the University of Alberta, Canada. His work is based on understanding the fundamentals of separation science, signal processing for chromatography, ion chromatography, HILIC, SFC, and ultrafast LC.

Daniel W. Armstrong is the Welch Distinguished Professor of Chemistry at the University of Texas at Arlington. Professor Armstrong has received more than 30 national and international research and teaching awards. His current interest involves chiral recognition, macrocycle chemistry, synthesis and use of ionic liquids, separation science, and mass spectrometry. He has more than 600 publications, one book, and 30 patents.

HILICON

iHILIC®-Fusion

advances HILIC separations in UHPLC and HPLC

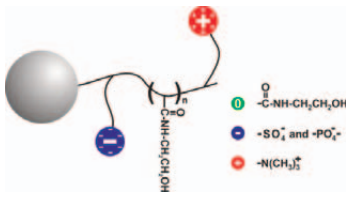

iHILIC®-Fusion
Silica based

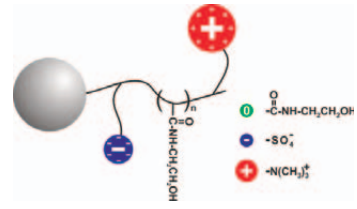

iHILIC®-Fusion(+)
Silica based

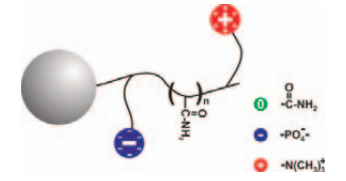

iHILIC®-Fusion(P)
Polymer based

- Charge modulated hydroxyethyl amide/amide HILIC columns
- Three complementary selectivities for separation of polar analytes
- Excellent durability and ultra-low bleeding for LC-MS
- Versatile columns for "Omics" studies and other applications
- iHILIC®-Fusion and iHILIC®-Fusion(+): pH 2-8; 1.8, 3.5, and 5 µm
- iHILIC®-Fusion(P): pH 1-10; 5 µm

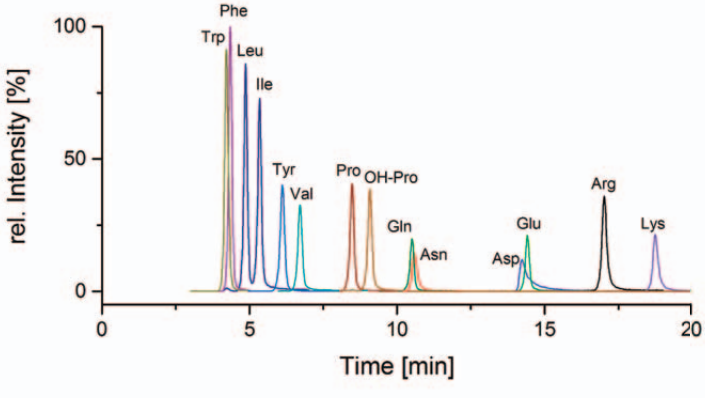

Meet us at:

ASMS 2018, June 3-7, 2018, San Diego, CA | Nordic Metabolomics Conference, Aug. 26-28, 2018, Örebro, Sweden

For more information:

Email: info@hilicon.com | Website: www.hilicon.com

Peak Purity in Liquid Chromatography, Part 2: Potential of Curve Resolution Techniques

Daniel W. Cook[1], Sarah C. Rutan[1], C.J. Venkatramani[2], and Dwight R. Stoll[3], [1]Virginia Commonwealth University (VCU), Richmond, Virginia, USA, [2]Genentech USA, San Francisco, California, USA, [3]LC Troubleshooting Editor

Is that peak "pure"? How do I know if there might be something hiding under there?

In part 1 of this series we discussed how the peak purity tools commonly provided in chromatographic data system software could aid in the detection of impurities in liquid chromatographic analysis (1). Here, we go one step further, and explore how a class of chemometric techniques known as *curve resolution methods* can be used to differentiate between a target compound and impurities, and subsequently quantify them, even when their peaks are overlapped.

As in the previous instalment (1), we focus on diode-array detection in liquid chromatography (LC–DAD). While mass spectrometric detection undoubtedly gives more selective information in the vast majority of cases, it is clearly a more complex detection mode and is prone to effects that can hamper quantitation such as ionization suppression because of matrix effects. The potential for highly precise quantitation of low-level impurities using DAD data is actually quite good, provided the spectra of the impurities have significantly different spectroscopic signatures as compared to the main peak. The latter point is of course an important caveat.

Multivariate Curve Resolution-Alternating Least Squares

In part 1 of this series we discussed the power of utilizing all of the absorbance information provided by a diode-array detector at multiple wavelengths to assess peak purity (1). Chemometric curve resolution techniques take this one step further. These techniques analyze the matrix of absorbance measurements at all wavelengths (that is, spectra) at all time points across a given time region of the chromatogram. Using a regression-based approach to determine how the spectra change over time, any impurities cannot only be discovered, but also be mathematically resolved from the target peak.

Using a regression-based approach to determine how the spectra change over time, any impurities cannot only be discovered, but also be mathematically resolved from the target peak.

Here we illustrate one of the most popular curve resolution techniques, known as *multivariate curve resolution-alternating least squares* (*MCR-ALS*) (2–6). The basis for this technique is a multicomponent formulation of Beer's law given as:

$$A_\lambda = \varepsilon_{\lambda,X} b c_X + \varepsilon_{\lambda,Y} b c_Y \quad [1]$$

where A_λ represents the measured absorbance of a mixture solution at wavelength λ, b is the detection pathlength, $\varepsilon_{\lambda,X}$ and $\varepsilon_{\lambda,Y}$ represent the molar absorptivities at this wavelength for two chemical species X and Y, and c_X and c_Y represent the concentrations of these species in the solution. For a two-component mixture, if absorbance measurements are obtained at two different wavelengths, and the molar absorptivities are known, it is possible to solve for the concentrations of the two species, X and Y, in the mixture solution via simple algebra. If measurements at more than two wavelengths are available, least squares regression is needed to obtain the concentrations. It is important to note that the assumption that the two (or more) signals are linearly additive is only valid in cases where the total signal is within the linear range of the detector (for example, at signals less than about 1500 mAU with DAD).

At this point, we generalize the discussion to a measurement x, and consider this as a signal in an LC–DAD chromatogram, such that the variable $x_{i,j}$ refers to the absorbance at the ith time point and jth wavelength of the chromatogram. Additionally, we consider the possibility that more than two chemical species may be present in the sample within the chromatographic peak, which gives the following expression:

$$x_{i,j} = c_{i,1}s_{1,j} + c_{i,2}s_{2,j} + \ldots c_{i,N}s_{N,j} \quad [2]$$

Here, $c_{i,n}$ refers to the concentration of species n at the ith time point in the chromatogram, and $s_{n,j}$ refers to the molar absorptivity-pathlength product for species n at the jth wavelength. The full spectrochromatogram can be easily understood in terms of a matrix product. In matrix notation, equation 2 is commonly written as

$$\mathbf{X} = \mathbf{CS}^{T} \quad [3]$$

A clear advantage to handling multiple chromatograms simultaneously is that calibration information and estimates of unknown concentrations can be obtained very efficiently.

where the rows and columns of matrix **X** represent the absorbance at each wavelength and time point, respectively, and the superscript T refers to the matrix transpose. This concept is illustrated schematically in Figure 1. If the molar absorptivities are known at all measured wavelengths for all species present in the peak, then it is straightforward to solve for the resolved chromatograms, **C**, as follows:

$$\mathbf{C} = \mathbf{X}(\mathbf{S}^{T})^{\dagger} \quad [4]$$

where the superscript † indicates the pseudo inverse operation. Equation 4 is simply a linear regression equation in matrix format. The columns of **C** are the individual component chromatograms (that is, each compound plus any background contributions), and the rows of $\mathbf{S}^{T}$ are the individual component spectra.

While in theory this approach could be a means of resolving overlapped chromatographic peaks, if there are unknown impurities present or uncharacterized mobile phase background components or species, then we do not have enough information to specify the **S** matrix. The MCR-ALS technique then becomes quite useful in this regard. Rather than exactly specifying **S**, an initial estimate for **S** is provided to the regression. This initial estimate can be obtained in a number of different ways. Pure variable methods are frequently used for this purpose. These methods seek to find the N most different spectra from the chromatographic data matrix, **X**, where N is the number of components needed to describe the measured data. The principle is that the most different spectra in the matrix are likely to be similar to the underlying pure component spectra. The caveat is that the number of components must be set by the user. Methods have been proposed for selecting the correct number of components such as scree plots; however, the only reliable method is evaluation of the results for multiple values of N. For a simple impurity screen, running MCR-ALS with two and three components to start should suffice, as one component would represent background, one would represent the target analyte, and if a third component is necessary, it is most likely because of an impurity peak.

Once this estimate for **S** is obtained, equation 4 is used to solve for the

Figure 1: Schematic for resolution of a spectrochromatogram represented by a matrix, **X**, into two component chromatograms and spectra contained by matrices **C** and **S**, respectively.

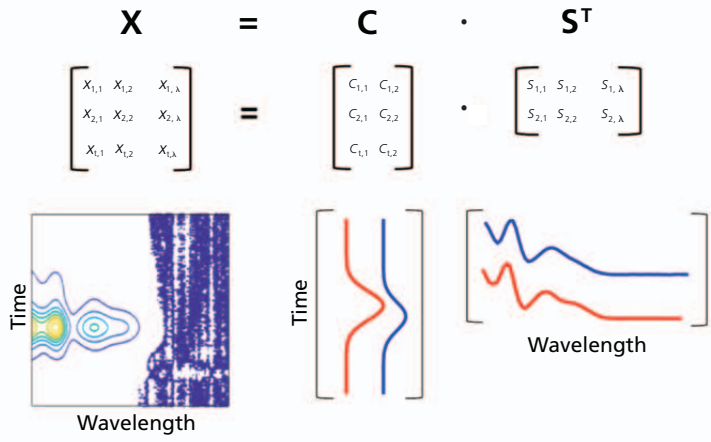

Figure 2: (a) Chromatogram of impure peak at 212 nm; (b) representation of this chromatogram as a contour plot where the *y*-axis is the UV-visible absorbance spectrum axis and the *x*-axis is the chromatographic time axis; (c) three most "pure" spectra within the spectrochromatogram found at the points circled in (a).

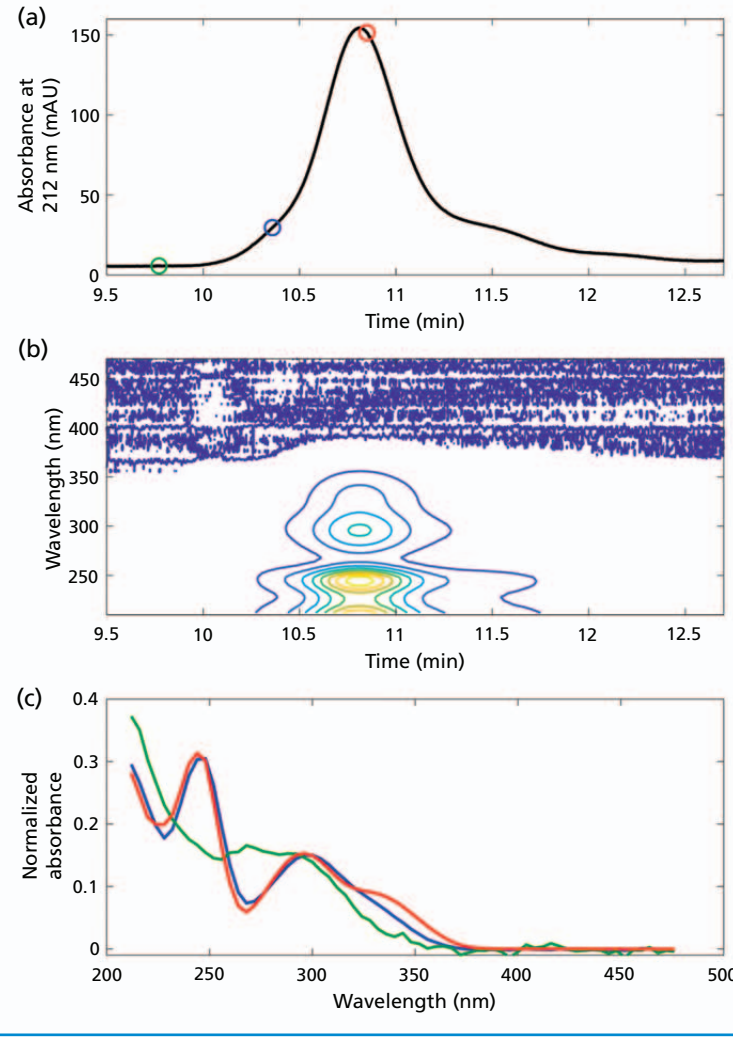

chromatographic profile matrix, **C**. Because the matrix **S** is only an approximation, **C** will only be an approximation as well. MCR-ALS can be considered an optimization method in which these **C** and **S** matrices are continuously improved with the goal of accurately representing the true underlying chromatographic and spectral profiles of each component. The power of MCR-ALS lies in the judicious implementation of constraints on the **C** matrix (and in subsequent steps, the **S** matrix as well) during this optimization. One frequently applied constraint is non-negativity, which allows the user to force the chromatographic profiles contained in **C** to have only positive values (6,7). Another constraint is unimodality, which forces each individual species chromatogram to exhibit a single peak (7). Many other constraints have been developed for MCR-ALS, but they are too numerous to describe here. Once **C** is constrained appropriately, the spectral matrix is updated via linear regression using equation 5:

$$\mathbf{S}^T = \mathbf{C}^{\dagger}\mathbf{X} \qquad [5]$$

MCR-ALS is able to distinguish compounds with even small differences in spectra given a large enough S/N.

Now, constraints can be applied to this **S** matrix as well; non-negativity is frequently used in this case too. By updating the **S** and **C** matrices in an alternating fashion (that is, equations 4 and 5), interspersed with the application of constraints, the final solutions for **C** and **S** will contain the pure component profiles of the individual chemical species within the chromatographic peak.

Application of MCR-ALS

We illustrate this approach using the chromatographic peak that was analyzed in part 1 of this series (1). Figure 2(a) shows the chromatographic peak, and Figure 2(b) shows the contour plot of the matrix **X**. We first applied a pure variable method (in this case the pure

method in the Barcelona MCR-ALS toolbox, based on the SIMPLISMA algorithm [8–10]), and selected the three most different spectra within the spectrochromatogram. The corresponding time points are shown as circles in Figure 2(a), and the three spectra at these points are shown in Figure 2(c). It is likely that the spectrum shown in green represents a background spectrum, because it corresponds to a spectrum appearing in the baseline (green circle at 9.77 min in Figure 2[a]). After these initial estimate spectra are submitted to MCR-ALS, it should allow the algorithm to estimate the background contribution to the data, as well as the chromatographic peaks for each chemical species present within the profile.

The performance of the MCR-ALS algorithm is highly dependent on the similarity of the spectra of the species contributing to the overlapped peak, as well as the signal-to-noise ratio (S/N) of the peaks.

The results for MCR-ALS analysis of this peak using these spectra for initial estimates are shown in Figure 3. Two peak shape responses within the chromatogram are resolved as shown in Figure 3(a). These are two of the components contained in the matrix **C**, corresponding to two chemical species (peaks shown in blue and red), and a background contribution from the mobile-phase gradient shown in green. The normalized spectra contained in matrix **S**, which correspond to these species or contributions, are shown in Figure 3(b). Note that the non-negativity constraint has been applied to the components corresponding to the real chemical species (shown in red and blue), while the background component (green) was not constrained. This flexible application of constraints leads to a powerful algorithm for curve resolution.

Quantitation with MCR-ALS: A natural limitation of the MCR-ALS algorithm in this case is that there generally are multiple mathematical solutions that satisfy equation 3. Constraints are used to limit the possible solutions, but this generally does not provide a unique, chemically valid solution, especially when using MCR-ALS to analyze a single chromatogram, as described above. An extension of the MCR-ALS technique to analyze multiple chromatograms simultaneously is quite powerful in this regard, especially for quantitative analysis. In this approach, the analyst runs a series of calibration sample mixtures with varying concentrations of the target analytes, and obtains chromatograms for test samples with unknown concentrations of the target analytes. Because MCR-ALS resolves signals resulting from individual chemical species, these calibration solutes are not required to be individual standards and can, in fact, be mixtures of the compounds of interest, minimizing the number of calibration samples that need to be analyzed. These measured spectrochromatograms are appended together along the time axis to form an

Figure 3: MCR-ALS results from the chromatogram shown in Figure 1. (a) Resolved pure component chromatograms; (b) resolved pure component spectra. The red and blue curves represent chemical species and the green curves represent background contributions.

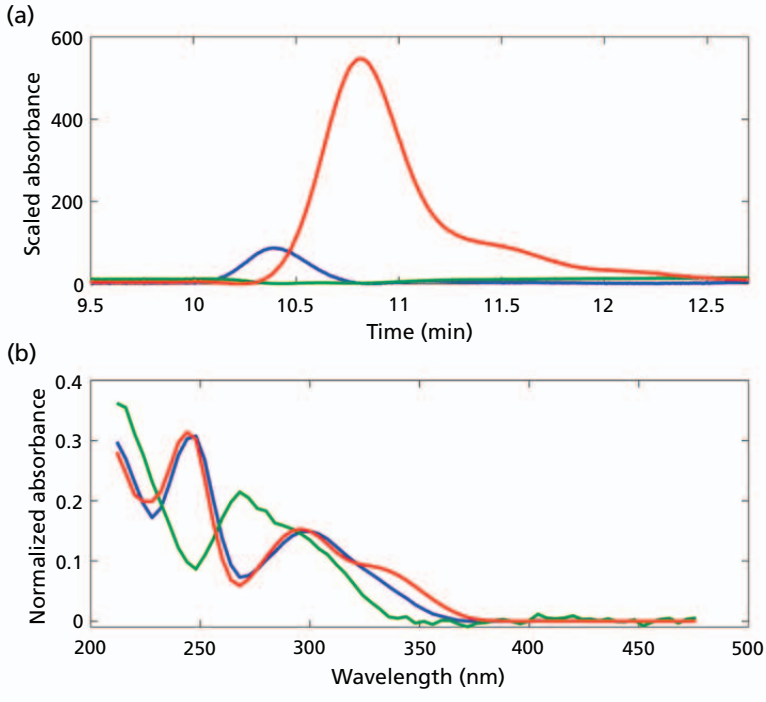

Figure 4: (a) Resolved chromatograms for five calibration mixtures (C1 through C5) containing psoralen and angelicin; table shows the corresponding concentrations; (b) Resolved spectra for psoralen (red), angelicin (blue), and a gradient background contribution (green).

Concentrations (ppm)

	C1	C2	C3	C4	C5	U1
Psoralen	50	5	10	20	1	?
Angelicin	5	1	50	20	10	?

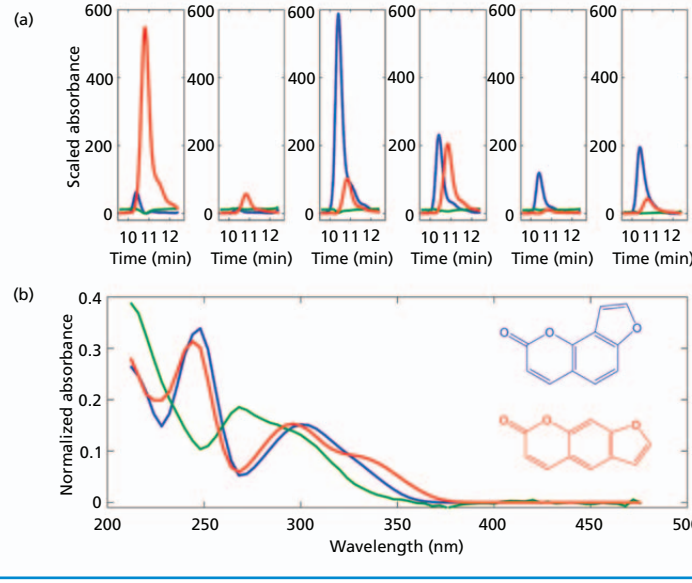

augmented matrix **X** as follows:

$$\mathbf{X} = \begin{bmatrix} \mathbf{X}_{c,1} \\ \mathbf{X}_{c,2} \\ \vdots \\ \mathbf{X}_{c,L} \\ \mathbf{X}_{u,1} \\ \mathbf{X}_{u,2} \\ \vdots \\ \mathbf{X}_{u,M} \end{bmatrix} \quad [6]$$

where the $\mathbf{X}_c$ are the L calibration chromatograms and the $\mathbf{X}_u$ are the M unknown chromatograms. MCR-ALS is carried out similarly to the approach described above. The resulting **S** matrix still consists of the N spectra of the pure component species, but the resulting **C** matrix now consists of $L + M$ resolved chromatograms for each of the N species, appended together similarly as shown in equation 6. The resolved chromatograms and spectra for a dataset of five calibration standards, C1–C5, and one unknown, U1, are shown in Figure 4 (that is, $L = 5$; $M = 1$). The table above the figure shows the known concentrations of the standard mixtures, and it can be seen that the scaled peak intensities in the chromatograms (Figure 4[a]) are proportional to these concentrations. By integrating these resolved chromatographic peaks, calibration curves can be constructed, as shown in Figure 5.

A clear advantage to handling multiple chromatograms simultaneously is that calibration information and estimates of unknown concentrations can be obtained very efficiently. Another advantage is the potential to add additional constraints to the analysis, which further limits the possible solutions for **C** and **S**. For example, if a blank chromatogram is included in the data set, the contributions of the chemical species for this chromatogram can be set to zero forcing the blank to be modelled using only the background components. Additionally, calibration constraints can be added to the analysis, which constrain the peak areas for the calibrated samples to follow an expected relationship between detector signal and concentration (11–13).

Of particular note here is the fact that two compounds present in the

Figure 5: Calibration curves for (a) psoralen and (b) angelicin from MCR-ALS results. Coloured circles indicate calibration points; black squares denote unknown sample points.

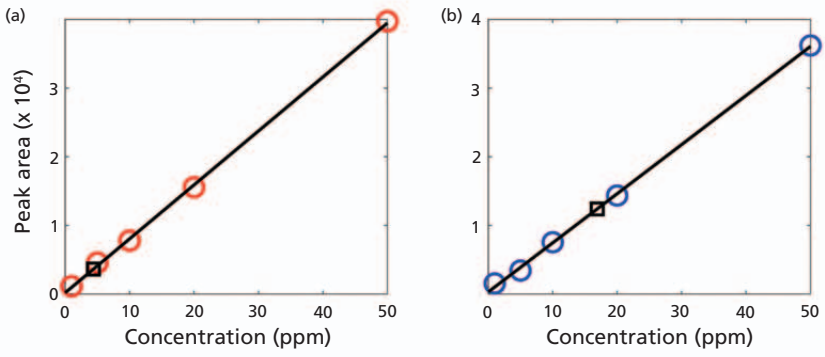

unknown sample have been reliably quantified, despite the resolution between the two peaks being significantly less than 1, and a high degree of similarity between their spectra. Here the chromatographic resolution of the two peaks is approximately 0.6.

Peak Capacity Enhancements via MCR-ALS

The performance of the MCR-ALS algorithm is highly dependent on the similarity of the spectra of the species contributing to the overlapped peak, as well as the signal-to-noise ratio (S/N) of the peaks. Here the similarity of the spectra for the two analytes psoralen and angelicin can be expressed by the correlation coefficient, which is 0.98 (see part 1 for further discussion).

The improvement of effective chromatographic performance can be quantified in terms of the peak capacity of the separation. The peak capacity of a gradient separation, n_c, can be estimated as follows:

$$n_c = \frac{t_{grad}}{w_b R_s'} \quad [7]$$

where t_{grad} is the time of the gradient, and w_b is the average width of the peaks at the base. The R_s' term is the resolution required for effective quantitative analysis (14). Typically, chromatographers use an R_s' value of 1 when calculating peak capacity. Clearly, if peaks can be quantified at a resolution of less than 1 using curve resolution as discussed above, then the effective peak capacity has been increased. In recent work, we have developed a quantitative relationship between peak capacity and the signal-to-noise ratio of neighbouring peaks and spectral similarity as measured by correlation coefficient. As an example, if the correlation coefficient between the overlapped spectra is 0.89 and S/N is 50, the chromatographic resolution required for quantitation is $R_s' = 0.3$. This results in a roughly threefold improvement in peak capacity relative to conventional use of DAD where the only means of separation is that provided by the column itself. Clearly, MCR-ALS can provide a significant enhancement in chromatographic method performance.

Availability of MCR-ALS in Software Packages

One hurdle to widespread usage of MCR-ALS is the lack of implementation of curve resolution options in commercial chromatographic data systems. Although commercial data systems for spectroscopy instruments (for example, infrared) frequently provide MCR-ALS or related curve resolution tools within their software, this situation is as not common for chromatographic data systems. To the best of our knowledge, only Shimadzu has recently added this capability to its data system software (15). The other option for chromatographers wishing to apply these methods to their data is to use one of the many available MCR-ALS toolboxes available for use in the Matlab programming

environment. Eigenvector Research, Inc. sells its PLS Toolbox package, which includes MCR-ALS (16). Matlab toolboxes are freely available from the Barcelona MCR-ALS group (10,17) and the Olivieri group (18), with the latter toolbox specifically focused on calibration applications. The Olivieri and Barcelona MCR-ALS toolboxes are also available for users without access to Matlab through a stand-alone graphical user interface (17,18). There is also an ALS package available for the open-source R statistical software environment (19).

Because of the lack of integration with instrumental software, an extra step is required to export the raw spectrochromatogram and read it into the third-party software packages listed above. Unfortunately, this approach is not always straightforward, depending on the instrument software. Although a few extra minutes may be required to move the data and to analyze with the third-party software, it will often require less time than it would take to analyze samples using different chromatographic columns or to vary other method parameters to resolve impurity peaks and increase confidence that none are present.

Concluding Remarks

To those of us who have utilized MCR-ALS for chromatographic analyses, it is clear that this technique adds a powerful tool to the chromatographer's arsenal. While the peak purity approaches described in part 1 of this series can identify whether impurities are present, MCR-ALS can resolve the pure chromatographic profile, allowing quantitation of the target analyte and the impurity if standards are available for the compound. As mentioned earlier, MCR-ALS does require that compound spectra be at least slightly different; however, MCR-ALS is able to distinguish compounds with even small differences in spectra given a large enough S/N as shown in Figure 3.

Here we have limited our discussion to impurity analysis in LC–DAD; however, it is worth noting that MCR-ALS finds use in many other analyses such as metabolomics and environmental analyses as well as other instrumental techniques from hyperspectral imaging to LC with mass spectrometric detection to two-dimensional liquid chromatography (3,4,20,21). The latter will be the focus of the next instalment in this series where we will look at how the additional separation dimension can help in the quest to determine peak purity particularly when spectrally indistinguishable impurities are present.

References

(1) S.C. Rutan, C.J. Venkatramani, and D.R. Stoll, *LCGC Europe* **31**(2), 74–81 (2018).

(2) A. de Juan and R. Tauler, *Crit. Rev. Anal. Chem.* **36**, 163–176 (2006).

(3) A. de Juan, J. Jaumot, and R. Tauler, *Anal. Methods* **6**, 4964–4976 (2014).

(4) D.W. Cook, M.L. Burnham, D.C. Harmes, D.R. Stoll, and S.C. Rutan, *Anal. Chim. Acta.* **961**, 49–58 (2017).

(5) S.C. Rutan, A. De Juan, and R. Tauler, in: *Comprehensive Chemometrics*, S. Brown, R. Tauler, and B. Walczak, Eds. (Elsevier, Oxford, UK, 2009), pp. 249–259.

(6) A. de Juan, S.C. Rutan, and R. Tauler, in: *Comprehensive Chemometrics*, S. Brown, R. Tauler, and B. Walczak, Eds. (Elsevier, Oxford, UK, 2009), pp. 325–344.

(7) A. de Juan, Y. Vander Heyden, R. Tauler, and D.L. Massart, *Anal. Chim. Acta.* **346**, 307–318 (1997).

(8) W. Windig, *Chemom. Intell. Lab. Syst.* **36**, 3–16 (1997).

(9) F.C. Sánchez and D.L. Massart, *Anal. Chim. Acta.* **298**, 331–339 (1994).

(10) R. Tauler, A. de Juan, and J. Jaumot, https://mcrals.wordpress.com/download/ (accessed 1 January 2018).

(11) G. Ahmadi, R. Tauler, and H. Abdollahi, *Chemom. Intell. Lab. Syst.* **142**, 143–150 (2015).

(12) R.R. De Oliveira, K.M.G. De Lima, A. De Juan, and R. Tauler, *Talanta* **125**, 233–241 (2014).

(13) A.C. de O. Neves, R. Tauler, and K.M.G. de Lima, *Anal. Chim. Acta.* **937**, 21–28 (2016).

(14) J.M. Davis and P.W. Carr, *Anal. Chem.* **81**, 1198–1207 (2009).

(15) S. Arase, K. Horie, T. Kato, A. Noda, Y. Mito, M. Takahashi, and T. Yanagisawa, *J. Chromatogr. A* **1469**, 35–47 (2016).

(16) http://www.eigenvector.com/software/pls_toolbox.htm (accessed 1 January 2018).

(17) J. Jaumot, A. de Juan, and R. Tauler, *Chemom. Intell. Lab. Syst.* **140**, 1–12 (2015).

(18) S.J. Mazivila, S.A. Bortolato, and A.C. Olivieri, *Chemom. Intell. Lab. Syst.* **173**, 21–29 (2018).

(19) K.M. Mullen, https://cran.r-project.org/web/packages/ALS/ALS.pdf (accessed 1 January 2018).

(20) D.W. Cook and S.C. Rutan, *Anal. Chem.* **89**, 8405–8412 (2017).

(21) J.M. Prats-Montalbán, A. de Juan, and A. Ferrer, Chemom. *Intell. Lab. Syst.* **107**, 1–23 (2011).

Dwight R. Stoll is the editor of "LC Troubleshooting". Stoll is an associate professor and co-chair of chemistry at Gustavus Adolphus College in St. Peter, Minnesota, USA. His primary research focus is on the development of 2D-LC for both targeted and untargeted analyses. He has authored or coauthored more than 50 peer-reviewed publications and three book chapters in separation science and more than 100 conference presentations. He is also a member of *LCGC*'s editorial advisory board. Direct correspondence to: LCGCedit@ubm.com

Sarah C. Rutan is a professor of chemistry at Virginia Commonwealth University (VCU), in Richmond, Virginia, USA, where she has been on the faculty for 33 years. Her research spans a broad range of areas in analytical chemistry and chemometrics, and is currently focused on the development of chemometric methods for improving chromatographic analyses, especially comprehensive 2D chromatography. She has more than 100 publications and numerous presentations on these topics.

C.J. Venkatramani is a senior scientist at Genentech USA and has more than 15 years experience in the pharmaceutical industry. He was the key member of Genentech technical team instrumental in the successful launch of gRed's first small molecule Erivedge, leading from development to commercial. His areas of interest include multidimensional chromatography and ultratrace analysis of genotoxic impurities.

Daniel W. Cook is a postdoctoral fellow in the pharmaceutical engineering laboratory within the Chemical and Life Science Engineering Department at Virginia Commonwealth University in Richmond, Virginia, USA. In this role, he serves as the primary analytical chemist for the research efforts of the Medicines for All Institute. He received his BS from Randolph-Macon College in 2011 and his Ph.D. in 2016 from Virginia Commonwealth University for his work focusing on the development and application of chemometric techniques to chromatography, particularly comprehensive 2D-LC.

VICI *Engineering the future of analytical science for 50 years*

Understanding how products are applied in the real world is the key to knowing how to make improvements.

Founder and President of VICI and affliated companies VICI DBS, VICI Valco, VICI Metronics, VICI Precision Sampling, and VICI AG, Stan Stearns began his career in science as a chemist in a crime lab, then in service and chromatographic applications for Wilkins in 1965 until it's purchase by Varian. Crossing real world experience with his technical knowledge gained at Wilkins, Stan invented solutions that would make an impact across industries, discovering new ways to apply and eventually improve analytical instruments.

1960s

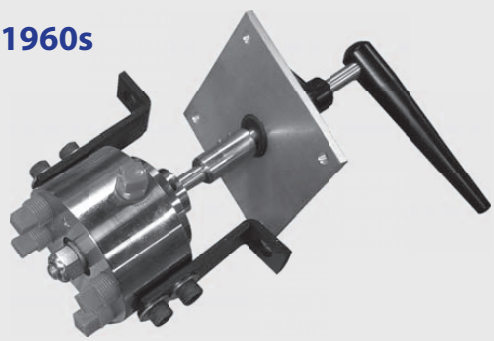

An insatiable curiosity started with improving valves, eventually driving analytical science to go where it never had been before. 50 years of pioneering the development of smaller and more efficient components and instruments, VICI now produces more than ten thousand different parts and products, still unrivaled in selection and technology.

1990s

What began as Valco Instruments in 1968, became VICI (Valco Instruments Company Incorporated), a legacy dedicated to analytical science 50 years later.

Today

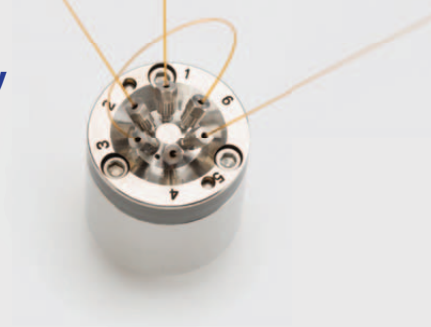

www.vici.com

Monitoring of Oxidation in Biopharmaceuticals with Top-to-Bottom High Performance Liquid Chromatography–Mass Spectrometry Methodologies: A Critical Check

Therese Wohlschlager, Christof Regl, and Christian G. Huber, Department of Biosciences, Bioanalytical Research Labs and Christian Doppler Laboratory for Biosimilar Characterization, University of Salzburg, Salzburg, Austria

Federal regulations concerning the safety and efficacy of biopharmaceuticals require the implementation of a comprehensive toolbox of physicochemical and biological characterization methods. In order to demonstrate consistent overall structure, even minute differences in primary structure and post-translational modifications (PTMs) have to be detectable in therapeutic proteins. Because of their remarkable capability of revealing small changes in molecular structure, high performance liquid chromatography (HPLC) and mass spectrometry (MS) rate among the most powerful technologies for comprehensive protein analysis. This article details the potential of both methods with regard to revealing methionine oxidation, a chemical modification that may be induced during downstream processing and storage of biopharmaceuticals. The benefits and limitations of bottom-up, middle-down, and top-down HPLC–MS analysis will be demonstrated for the detection of oxidation variants in a therapeutic monoclonal antibody (mAb).

Seven of the ten top-selling pharmaceuticals in 2016 were protein therapeutics (1), which are usually manufactured in a biotechnological process involving cell culture (2). Very stringent safety regulations by the health authorities mandate elaborate analytical schemes for the comprehensive characterization of the efficacy and safety of pharmaceutical products. This is even more valid for protein therapeutics (3) because the large molecular size and unavoidable variances in biosynthesis and downstream processing may result in molecular variants with regard to amino acid sequence, three-dimensional protein structure, post-translational modifications (PTMs), or process-related artificial modifications, all of which may impact therapeutic efficacy and safety (4). In this context, nonenzymatic oxidation of proteins at methionine residues resulting in methionine–sulfoxide or methionine–sulfone represents one of the most relevant protein degradation reactions (5). Oxidation of methionines has been shown to significantly influence the biological activity of proteins (6), hence limiting the stability and shelf life of protein-based pharmaceuticals (7–10).

Developed in the mid-1960s initially for the separation of small molecules (11), high performance liquid chromatography (HPLC) has been adapted to the separation of high molecular biopolymers (12) upon implementation of dedicated stationary phase configurations enabling rapid mass transfer, such as sub-2-µm totally porous particles (TPPs), superficially porous particles (SPPs), or monolithic phases. Likewise, progress in mass spectrometry (MS) technologies, especially electrospray ionization (ESI) for biopolymers (13), as well as high-resolution mass analyzers such as time-of-flight (TOF) or orbital trap mass analyzers (14), have significantly contributed to the success of bioanalytical methods in pharmaceutical analysis. This article will shed light on the potential, challenges, and achievements of HPLC in combination with ESI-MS for the analysis of therapeutic proteins with an emphasis on protein oxidation, which represents a relatively minute modification at the level of primary structure. Oxidation, however, generally entails serious consequences in three-dimensional protein structure and biological activity, rendering its

Figure 1: Structural levels for the characterization of monoclonal antibodies (mAbs). For details see main text.

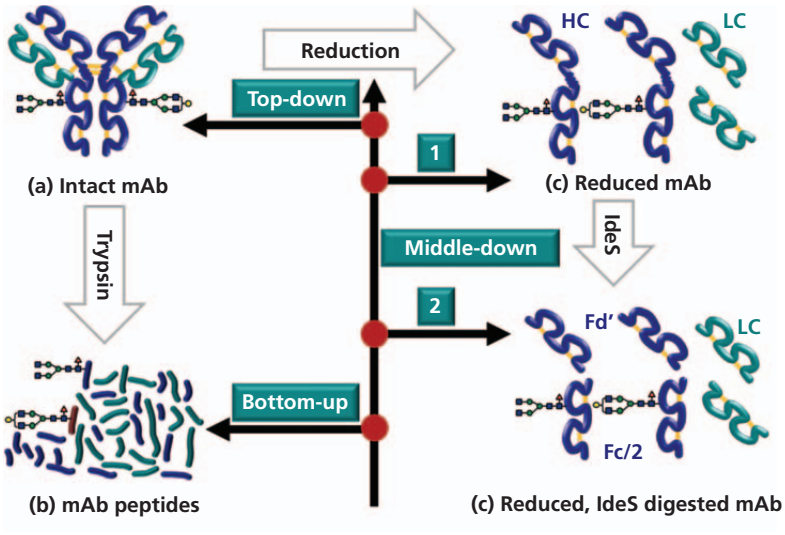

Figure 2: Simulation of isotopic patterns and isotopic envelopes for charge state 1+ of (a) an intact mAb, (b) heavy chain (HC), and (c) Fc/2. Full resolution of isotope signals for a 150 kDa molecule requires a mass spectrometric resolution of 560,000 (a), while isotope signals of a 25 kDa fragment are resolvable at a resolution of 140,000 (c); 1:1 relates to the relative concentration of both species.

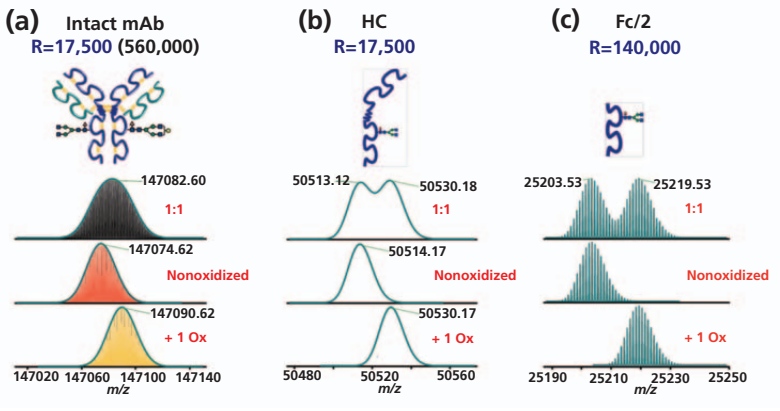

diligent characterization mandatory in biopharmaceutical analysis.

Structural Levels of Protein Characterization: Fundamental Considerations: Using an antibody molecule as an example, Figure 1 illustrates the structural levels that may be relevant for protein characterization in a biopharmaceutical context. Traditionally, the analysis of protein sequence and PTMs is performed after digestion with a protease, yielding a specific set of peptides (Figure 1[b]) that is analyzed by HPLC and MS. This approach is termed bottom-up analysis, offering the advantage that even small changes in a peptide, for example, an additional oxygen atom, entail a large relative change in the physicochemical properties of the peptide, which may be readily detectable by HPLC and MS.

For example, oxidation of DTLMISR, a methionine-containing peptide of the therapeutic antibody rituximab, results in a mass shift from 834.4269 to 850.4218 Da, representing a relative mass

Figure 3: Separation of tryptic peptides of oxidatively stressed rituximab. (a) Total ion current chromatogram, (b) extracted ion current chromatograms at *m/z* 835.4373, and (c) 851.4322, respectively. Fragment ion spectra of (d) nonoxidized and (e) oxidized DTLMISR peptide. Column: 100 × 1.0 mm, 1.9-µm Hypersil Gold aQ (Thermo Fisher Scientific); gradient: 2.0% acetonitrile in 0.10% aqueous trifluoroacetic acid for 5.0 min, 5.0–10% in 5.0 min, 10–40% in 60 min, 100% for 5.0 min, 2% for 25 min, 60 µL/min; sample: 5.0 µg of rituximab stressed with 0.30% hydrogen peroxide. The extracted ion current chromatograms show the traces for nonoxidized and oxidized peptide DTLMISR of the HC of rituximab at RT 33.13 and 29.59 min, respectively. For experimental details, see reference 9.

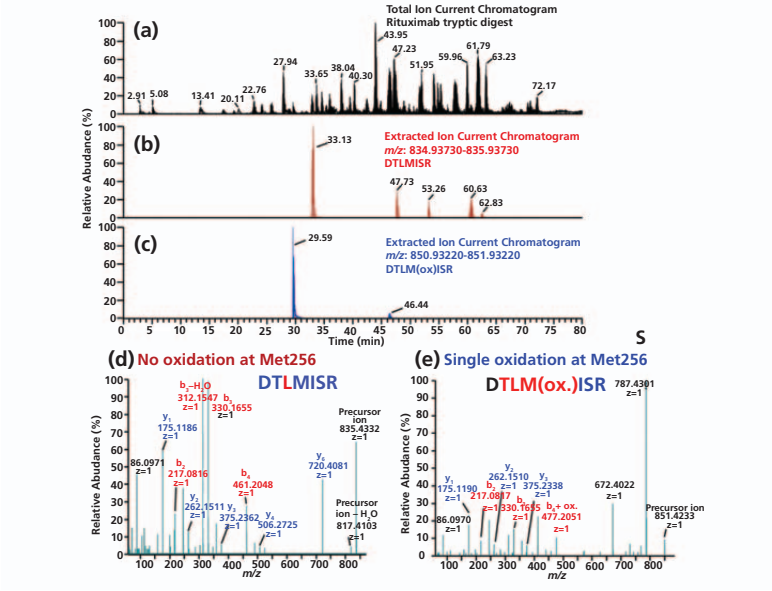

Figure 4: Investigation of mAb oxidation at the intact protein level. (a) Total ion current chromatogram of control (red trace) and stressed (blue trace) rituximab, (b) mass spectra extracted at different elution times of stressed rituximab (b). Column: 150 × 2.1 mm, 4-µm MAbPac RP (Thermo Fisher Scientific); gradient: 31.5–33.2% acetonitrile in 0.050% aqueous trifluoroacetic acid in 7 min, 200.0 µL/min, 80 °C; detection: Q Exactive (Thermo Fisher Scientific); HESI +4.0 kV; ISF: 80.0 eV; full scan 1800–5000 *m/z* at R = 17,500; sample: 1000 ng rituximab control and treated with 0.35% hydrogen peroxide for 30 min at 22 °C.

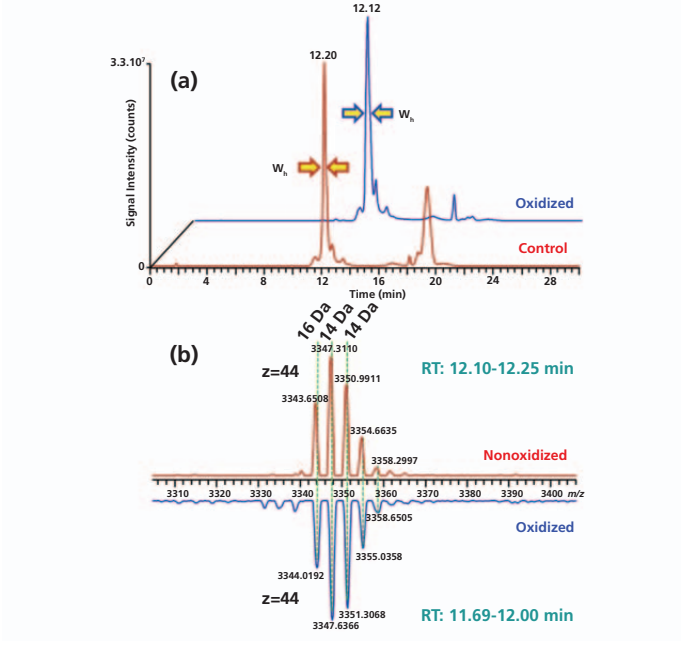

difference of 1.88% that can readily be distinguished by MS. Moreover, incorporation of an additional oxygen atom into the peptide will decrease its hydrophobicity, which may facilitate the separation of oxidized and nonoxidized peptide variants by reversed-phase HPLC. Finally, sequence information may be gained upon gas-phase fragmentation and detection of fragment ions by MS, enabling both the identification and localization of modifications of specific amino acids. Apart from being laborious, time-consuming, and prone to the introduction of artifacts during proteolytic digestion, the bottom-up approach is limited in that the context of modifications within the different intact molecular protein species is lost.

On the other hand, protein analysis may be attempted at the intact molecule level, as realized in so-called top-down approaches (Figure 1[a]). Numerous examples have successfully shown that therapeutic mAbs may efficiently be analyzed as intact proteins using HPLC and MS methods (15,16). Studies on the gas-phase fragmentation have also demonstrated that a considerable amount of sequence information may be collected from fragments generated from intact proteins by collision-induced dissociation (CID), electron capture dissociation (ECD), or electron-transfer dissociation (ETD) (17). Nevertheless, subtle changes in protein structure may be difficult to detect as a result of limitations in chromatographic or mass spectrometric capabilities to discern the change. To stay with the example given above, incorporation of one oxygen atom into an intact mAb molecule will result in a mass shift from 147074.62 to 147090.62 Da (+16 Da), representing a relative mass difference of 109 ppm, which is well within the typical mass accuracies of modern TOF and orbital trap mass spectrometers. Simulation of the isotopic patterns of two mAb species differing in a single oxygen atom, however, shows that the isotopic envelopes merge into a single broad distribution even at a mass spectrometric resolution sufficient to separate neighbouring isotope peaks. Thus, distinction of oxidized- and

Figure 5: HPLC–MS analysis of LC and HC derived from control (red trace) and stressed (blue trace) rituximab. (a) Total ion current chromatogram, (b, c, d) mass spectra extracted at different elution times of HC derived from stressed rituximab, (e) mass spectrum extracted for full width HC peak derived from stressed rituximab. Column: 150 × 2.1 mm, 4-µm MAbPac RP (Thermo Fisher Scientific); gradient: 32.0–32.5% acetonitrile in 0.10% aqueous trifluoroacetic acid in 12.5 min, 150 µL/min, 80 °C; detection: Q Exactive (Thermo Fisher Scientific); HESI +4.0 kV; ISF: 80.0 eV; full scan, 0–8.5 min 700–2500 *m/z* at R = 140,000, 8.5–19.0 min 800–3500 *m/z* at R = 17,500; sample: 150 ng rituximab control and treated with 0.30% hydrogen peroxide for 30 min at 22 °C and reduced with 20 mM dithiothreitol for 30 min at 37 °C.

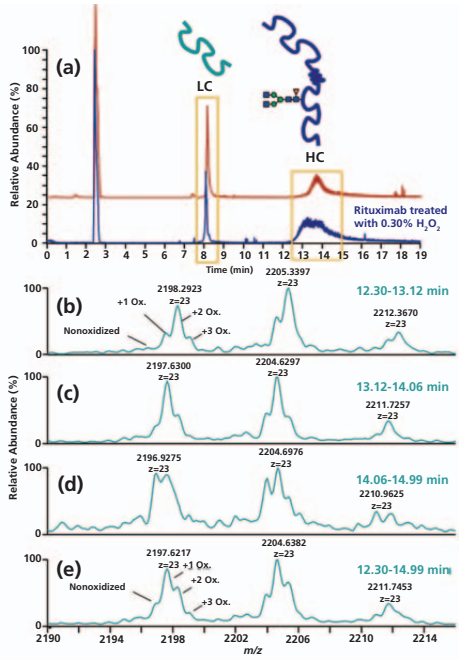

nonoxidized mAb species by MS at the intact protein level is not feasible (Figure 2[a]).

In order to obtain smaller protein subunits for investigation, tetrameric antibody molecules can be dissociated into two heavy and two light chains (HC and LC, respectively) by reduction of intermolecular disulfide bonds, yielding two 25 kDa LC and two 50 kDa HC subunits. While the isotopic patterns of the HC molecules are still not completely resolvable by MS (Figure 2[b]), the width of the isotopic pattern of a 25 kDa fragment is narrow enough to facilitate clear separation of oxidized- and nonoxidized species (demonstrated for a 25 kDa Fc/2 fragment in Figure 2[c]). Such fragments can be obtained upon proteolytic digestion with papain or IdeS, which specifically cleave within the so-called hinge region of the HC (Figure 1[d]). The two resulting fragments of almost identical size (Fd' and Fc/2; approximately 25 kDa each) are ideally suited for the analysis of oxidation variants because they can readily be resolved by MS, especially as the main oxidation sites are located in the Fc domain (18).

Bottom-Up Determination of Antibody Oxidation at the Proteolytic Peptide Level: The classical approach to comprehensive protein characterization comprises chromatographic separation of proteolytic peptides by ion-pair (IP)-reversed-phase HPLC followed by sequence analysis of the separated peptides by tandem MS. Figure 3 illustrates that oxidation of methionine facilitates a clear chromatographic separation of the corresponding peptides. As expected, the incorporation of oxygen results in a decrease in hydrophobicity and hence a decrease in chromatographic retention of the oxidized variant of the peptide. Relative peak areas of the chromatographic peaks that are well separated may be used to relatively quantify the extent of oxidation at the peptide level. In addition, fragment spectra as shown in Figure 3(d) and 3(e) unambiguously identify the site of oxidation as methionine at position four of the peptide. Apart from oxidation monitoring, the high resolving power and mass accuracy of modern high-resolution mass spectrometers enables the detection of mass differences as little as 1 Da, which is characteristic for the deamidation of asparagine or glutamine residues, making peptide mapping one of the most powerful tools for the detection of protein modifications.

Investigation of Antibody Oxidation at the Intact Protein Level: As investigation of mAb oxidation at the intact protein level would eliminate the need for sample preparation by digestion and hence avoid oxidation artifacts, the separation of oxidized rituximab variants on a large-pore polymer-based column developed for the separation of mAbs was attempted. Comparison of the chromatographic profiles of control and stressed sample in Figure 4(a) reveals a slight decrease in retention time (by approximately 5 s) and an increase in the peak width at half height of the eluting peak profile for the oxidized protein (from 11 to 15

Figure 6: Chromatographic separation and mass spectrometric detection of Fc/2 derived from stressed rituximab with intramolecular disulfides (a) intact or (b) reduced. Mass spectra extracted for (c) doubly-oxidized, (d) mono-oxidized, and (e) nonoxidized Fc/2 (z = 10). Column: 150 × 2.1 mm, 4-µm MAbPac RP (Thermo Fisher Scientific); gradient: 28.9% acetonitrile in 0.10% aqueous trifluoroacetic acid for 5.0 min, 28.9–29.0% in 15 min, 29–30% in 9 min, 30–45% in 5 min, 100% for 5.0 min, 28.9% for 10 min, 200 µL/min, 80 °C; detection: Q Exactive (Thermo Fisher Scientific); HESI +3.5 kV; full scan: 1500–3000 *m/z* at R = 140,000; sample in (b–d), 500 ng rituximab treated with 0.35% hydrogen peroxide for 30 min at 22 °C, digested with IdeS, and reduced with 5 mM TCEP for 15 min at 60 °C. Adapted with permission from reference 9, Copyright 2017 American Chemical Society.

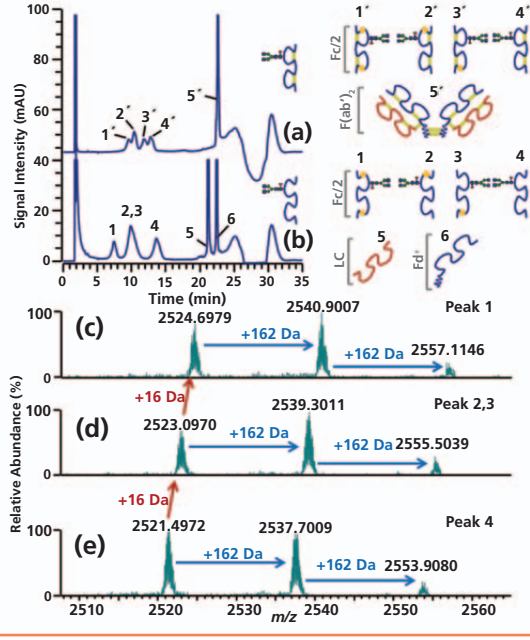

Figure 7: Fragment ion spectrum of singly oxidized Fc/2 (peak 2,3 in Figure 6[b]) obtained upon all ion fragmentation at 96 eV in the higher energy collision cell of a Q Exactive mass spectrometer. The diagnostic fragments b34 (red) for methionine residue Met256 and y45 (blue) for Met432 are annotated (a) in the raw spectrum and (b) in the sequence of Fc/2. Adapted with permission from reference 9, Copyright 2017 American Chemical Society.

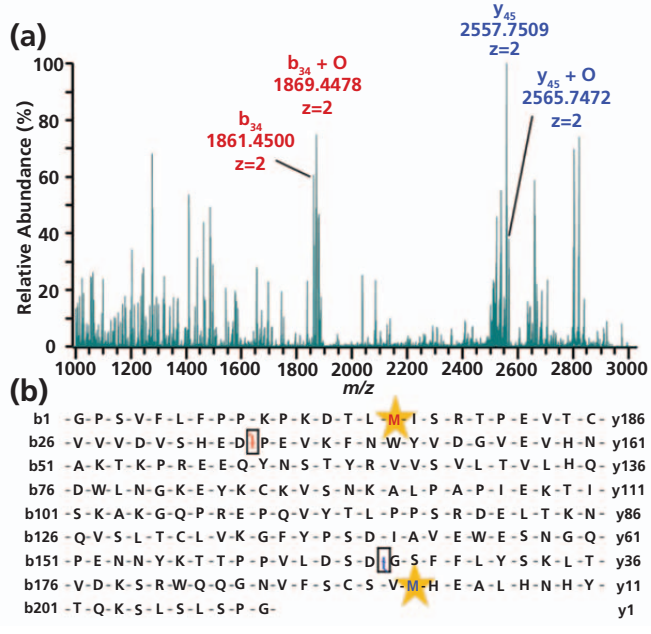

s). These effects can be attributed to reduced hydrophobicity of the oxidized protein variants as well as increased complexity of the sample because oxidation may occur at different sites, resulting in a range of diverse protein species. Nevertheless, oxidized mAb variants cannot even partially be separated from nonoxidized species by means of IP-reversed-phase chromatography.

The corresponding mass spectra reveal a shift towards higher molecular mass of the oxidized protein, as shown in Figure 4(b) for the 44+ charge state of rituximab consisting of multiple signals that arise from the different glycoforms. When comparing corresponding glycoforms of oxidized and control samples, shifts in the range of *m/z* 0.32–0.37 translating into mass differences of 14–16 Da are detectable. Again, resolution of signals for different oxidized mAb species is impossible and the masses observed for the stressed sample represent averages of different singly- and multiply-oxidized protein variants, rendering the approach not viable for the exact determination of protein oxidation.

Investigation of Antibody Oxidation in the HC: Moving one step down from the intact protein level of an antibody, Figure 5 depicts the HPLC–MS analysis of LC and HC derived from a control and an oxidatively-stressed rituximab sample. LC and HC were efficiently separated when eluted with a very shallow gradient of 32.0–32.5% acetonitrile in 12.5 min. When compared to the control sample, significant broadening of the chromatographic peak corresponding to oxidized HC was observed, indicating partial separation of different oxidized species (Figure 5[a]), although separation into discrete peaks was not attainable. Extraction of mass spectra from different time intervals within the chromatographic peak revealed that higher oxidized species, as evidenced by higher mass, eluted earlier compared to mono- or nonoxidized HC species (Figure 5[b–e]). Incorporation of up to three oxygen atoms, consistent with the occurrence of three methionines in the HC sequence, was observable in the mass spectra. Nevertheless, mass spectral resolution of the

different oxidation variants allowing their unambiguous differentiation and quantification was still not feasible.

Investigation of Antibody Oxidation in the Fc/2 fragment: Finally, the analysis of methionine oxidation was performed in Fc/2 generated upon proteolysis with IdeS, an enzyme cleaving within the hinge region of the HC sequence. Interestingly, when intramolecular disulfide bridges in the HC domain were kept intact, a separation of four oxidized variants of Fc/2 (one nonoxidized, two singly-oxidized, one doubly-oxidized species) was observable (Figure 6[a]). On the other hand, the two mono-oxidized Fc/2 species coeluted after the intermolecular disulfide bridges were cleaved upon reduction (Figure 6[b]). This observation suggests that changes in the three-dimensional structure induced by methionine oxidation play an important role in the chromatographic separation of oxidized proteins or protein fragments (8–10). Moreover, the baseline separation of non-, mono- and doubly-oxidized species enabled the quantitative determination of oxidized protein variants both by UV-spectroscopic and mass spectrometric detection with relative process standard deviations between 7 and 14% (9). MS not only confirmed the +16 Da mass shifts as a result of the incorporation of oxygens (Figure 6[c–e]), but also allowed the localization of oxidation sites by middle-down fragmentation of Fc/2 (Figure 7).

Conclusions

The ability of analytical technologies to distinguish between oxidized and nonoxidized protein species is limited by several factors. Bottom-up analysis of tryptic peptides facilitates detailed analysis of even minor modifications and simultaneously provides sequence information deduced from tandem MS experiments. Nevertheless, the context of the different modifications in the whole protein is undetectable in this analytical approach. At the intact protein or HC level, efficient separation of oxidation variants of IgG1 type mAbs by reversed-phase HPLC or IP-reversed-phase-HPLC is generally impossible, mostly because of the minimal differences in hydrophobicity upon incorporation of additional oxygen atoms. In mass spectrometry, the natural width of the isotopic pattern limits the capability to distinguish oxidized proteins from their nonoxidized analogues to molecules smaller than approximately 25 kDa. Thus, oxidation monitoring in therapeutic mAbs is possible after decomposition into light and heavy chains, followed by proteolytic cleavage of the heavy chain into two fragments of 25 kDa. Moreover, at this molecular scale, non-, mono-, and doubly-oxidized variants can be separated by IP-reversed-phase-HPLC.

Acknowledgement

The financial support by the Austrian Federal Ministry for Digital and Economic Affairs and by a start-up grant of the State of Salzburg is gratefully acknowledged.

Conflict of Interest Statement

Sandoz, a Novartis Division, and Thermo Fisher Scientific provide financial support for the Christian Doppler Laboratory for Innovative Tools for Biosimilar Characterization. The salary of Therese Wohlschlager is fully funded; Christian G. Huber's salary is partly funded by the Christian Doppler Laboratory for Biosimilar Characterization. The authors declare no other competing financial interest.

References

(1) J. Njarðarson, *http://njardarson.lab.arizona.edu/* Accessed 15 May 2018.
(2) M. Butler, *Applied Microbiology and Biotechnology* **68**, 283–291 (2005).
(3) A.J. Chirino and A. Mire-Sluis, *Nature Biotechnology* **22**, 1383–1391 (2004).
(4) X. Zhong and J.F. Wright, *International Journal of Cell Biology* **2013**, 19 (2013).
(5) N. Jenkins, L. Murphy, and R. Tyther, *Molecular Biotechnology* **39**, 113–118 (2008).
(6) H.S. Lu, P.R. Fausset, L.O. Narhi, T. Horan, K. Shinagawa, G. Shimamoto, and T.C. Boone, *Archives of Biochemistry and Biophysics* **362**, 1–11 (1999).
(7) I.C. Forstenlehner, J. Holzmann, K. Scheffler, W. Wieder, H. Toll, and C.G. Huber, *Analytical Chemistry* **86**, 826–834 (2014).
(8) I.C. Forstenlehner, J. Holzmann, H. Toll, and C.G. Huber, *Analytical Chemistry* web-published, (2015).
(9) C. Regl, T. Wohlschlager, J. Holzmann, and C.G. Huber, *Analytical Chemistry* **89**, 8391–8398 (2017).
(10) J. Holzmann, A. Hausberger, A. Rupprechter, and H. Toll, *Analytical and Bioanalytical Chemistry* **405**(21) 6667–6674 (2013).
(11) C. Horváth, B.A. Preiss, and S.R. Lipsky, *Analytical Chemistry* **39**, 1422–1428 (1967).
(12) F.E. Regnier and J. Kim, *Analytical Chemistry* **90**, 361–373 (2018).
(13) J.B. Fenn, M. Mann, C.K. Meng, S.F. Wong, and C.M. Whitehouse, *Science* **246**, 64–71 (1989).
(14) A. Makarov, *Analytical Chemistry* **72**, 1156–1162 (2000).
(15) J. Mohr, R. Swart, M. Samonig, G. Böhm, and C.G. Huber, *Proteomics* **10**, 3598–3609 (2010).
(16) A. Beck, S. Sanglier-Cianferani, and A. Van Dorsselaer, *Analytical Chemistry* **84**, 4637–4646 (2012).
(17) N. Bandeira, V. Pham, P. Pevzner, D. Arnott, and J.R. Lill, *Nature Biotechnology* **26**, 1336–1338 (2008).
(18) C. Chumsae, G. Gaza-Bulseco, J. Sun, and H. Liu, *J. Chromatogr. B Analyt. Technol. Biomed. Life Sci.* **850**, 285–294 (2007).

Therese Wohlschlager is a postdoctoral researcher at the University of Salzburg, Austria. Within the Christian Doppler Laboratory for Biosimilar Characterization she focuses on the development of analytical tools for the characterization of glycosylated biopharmaceuticals.
Christof Regl is a PhD student at the University of Salzburg and part of the Christian Doppler Laboratory for Biosimilar Characterization. His research project deals with the analysis of therapeutic mAbs ranging from bottom-up to top-down strategies.
Christian Huber trained as an analytical chemist at the University of Innsbruck and is currently a professor of chemistry for biosciences at the University of Salzburg. He also leads the Christian Doppler Laboratory for Biosimilar Characterization, which cooperates with Novartis and Thermo Fisher Scientific. His research interests include proteome and metabolome analysis as well as in-depth protein characterization by means of HPLC and MS.
Koen Sandra is the editor of "Biopharmaceutical Perspectives". He is the Scientific Director at the Research Institute for Chromatography (RIC, Kortrijk, Belgium) and R&D Director at anaRIC biologics (Ghent, Belgium). He is also a member of *LCGC Europe*'s editorial advisory board. Direct correspondence about this column to the editor-in-chief, Alasdair Matheson, at alasdair.matheson@ubm.com

Antibody–Drug Conjugates: Perspectives and Characterization

Rowan E. Moore[1], Kelly Broster[1], Ken Cook[1], Kyle D'Silva[1], Eric Niederkofler[1], Aaron O. Bailey[1], Jonathan Bones[2], and Michael W. Dong[3], [1]Thermo Fisher Scientific, Hemel Hempstead, United Kingdom, [2]National Institute of Bioprocessing Research and Training (NIBRT), Blackrock, Co. Dublin, Ireland, [3]Perspectives in Modern HPLC editor

This instalment of "Perspectives in Modern HPLC" provides an overview of antibody–drug conjugates (ADCs) as a new class of biotherapeutics and describes their analytical characterization for quality assessment with examples from extensive applications libraries.

Chemotherapeutic agents have been the mainstay of anticancer therapy since the early 1940s. Chemotherapy, or the use of cytotoxic agents in medical oncology to inhibit the process of mitotic cell division, is routinely administered with curative intent, to prolong life or as part of palliative care. Although the use of chemotherapy can result in a significant response—for example, in the treatment of testicular cancer—its use is associated with a range of adverse effects. Many of the adverse effects of chemotherapy are the result of damage to healthy cells that divide rapidly and are thus sensitive to antimitotic drugs.

Antibody–drug conjugates (ADCs) are an increasingly important class of biotherapeutics that utilize the specificity of monoclonal antibodies (mAbs) and the cytotoxicity of a potent anticancer payload (1–3). The two molecules are connected via chemical linkers, and the result is a therapy that is able to provide sensitive discrimination between healthy and diseased tissues. The antibody targets and binds to a selected antigenic cell-surface receptor that is, ideally, only expressed on the target cancer cell. After an ADC binds to its target cell, the cell internalizes the ADC through receptor-mediated endocytosis, and the cytotoxic payload is then released inside the lysosomal cellular compartment to provide precise, selective delivery to the cancerous cells. Payload conjugation typically takes place on the amino groups of lysine residues or the sulfhydryl groups of interchain cysteine residues as is the case in ado-trastuzumab emtansine (Kadcyla, Genentech/Roche) and brentuximab vedotin (Adcetris, Seattle Genetics/Millennium Pharmaceuticals), respectively. With 80–100 lysine residues and only eight interchain cysteine residues available in each mAb molecule, lysine conjugation yields a more heterogeneous mixture of species compared to cysteine-conjugated ADCs. Figure 1 depicts examples of common payload conjugation types, namely lysine, cysteine, and glycoconjugates (4).

In addition to the described primary amino acid structure, mAbs and ADCs also have distinct higher order structures that dictate their function and immunogenicity. They may be influenced by the above-described modifications and can appear as dimers or aggregates that also have the potential to induce immune responses and affect clearance rates.

For an ADC to demonstrate efficacy, it must incorporate a mAb that recognizes a specific tumour-associated antigen, a linker that has systemic stability but is specifically released at the target cell, and a cytotoxic agent that exhibits toxicity to the tumour cell as a stand-alone modality.

ADC Regulations

Whether submitting to the United States Food and Drug Administration (U.S. FDA), European Medicines Agency (EMA), or other regulatory bodies, ADC developers are covering new territory. Since ADCs incorporate both biologics and small-molecule moieties, these complex therapeutics are difficult to characterize, and multiple health authority experts are required to evaluate different aspects of the end product.

An ADC may be based on a previously approved mAb. For example, trastuzumab (Herceptin) is the mAb portion of the ADC Kadcyla. In such instances, new analytical technologies that have emerged since the development of the original mAb drug product should be evaluated for use in characterizing the related ADC. Consistent with the principles of quality by design (QbD), regulators expect sponsors to use the most current and effective technologies available to build product and process knowledge into controlling product quality.

With the approvals of Kadcyla, Adcetris, and more recently inotuzumab ozogamicin (Besponsa, Pfizer), gemtuzumab ozogamicin (Mylotarg, Pfizer), and more than 50 ADCs in clinical trial pipelines, the clinical application of ADCs is accelerating rapidly (5).

It is important to have a clear understanding of the relationship between the conjugation and manufacturing process, and the resulting product quality and heterogeneity of the ADC. The potency of an ADC is due, in part, to the extent of drug-linker incorporation on the mAb. Methods that can structurally characterize the drug load and distribution have been developed and proven to be critically important for understanding ADC product quality. Wakankar and colleagues have summarized several considerations

for the development of analytical methods that measure quality attributes unique to ADCs, such as drug load and drug distribution (6). In addition, several articles documenting the analytical strategies (7) as well as chromatographic and electrophoretic techniques for the characterization of ADCs have been published (8–10).

Characterization and Quality Control Requirements

Quality control (QC) testing of an ADC needs to account for its identity, purity, concentration, and activity (potency or strength)—the same as for any other biopharmaceutical product. Because of the inherent structural complexity of mAbs along with the covalently linked cytotoxic agents, several QC tests are required (8–10). A full understanding of the manufacturing process and its effect on the physicochemical and biological attributes of an ADC must be ascertained. However, in the case of ADCs, even the well-established QC terminology is not straightforward—for instance, the terms *potency* and *strength* have different meanings depending on whether the molecule being developed is large or small. The International Conference on Harmonization of Technical Requirements for Registration of Pharmaceuticals for Human Use (ICH) Q6A for small molecules lists strength (or assay) as a measure of the amount of an active pharmaceutical ingredient (API) (11). ICH Q6B for large molecules uses the term potency as a quantitative measure of biological activity (12). For an ADC that includes both of these components, total function (or potency) would need to be measured with a cell-based assay that assesses overall structure, antigen binding, drug loading, and drug delivery.

Unlike their pharmaceutical predecessors and more straightforward protein-based therapeutics, there is limited availability of certified standards for ADC test method development or comparison. Recently, Merck launched SigmaMAb Antibody-Drug Conjugate Mimic for use as a standard for mass spectrometry (MS) and high performance liquid chromatography (HPLC). SigmaMAb is an "ADC mimic" that conjugates SigmaMab (MSQC4), an IgG1 mAb, to dansylcadaverine fluorophores via a succinimidyl-4-(*N*-maleimidomethyl) cyclohexane-1-carboxylate (SMCC) crosslinker (13). At this time, the onus is completely on the developers to devise and implement a set of critical tests for identity and purity, involving the most appropriate analytical technologies. Each intermediate (mAb, linker, and drug) should have a reference standard in addition to an ADC reference standard, to be used in designated release and stability tests. These standards are critical reagents used for analytical method system suitability and in characterization, stability, and bridging studies, as is currently expected for all pharmaceutical and biopharmaceutical products. The cohort of tests would be performed as part of chemistry, manufacturing, and control (CMC) efforts during drug development. Many of these tests would become assays for critical quality attributes (CQA) or analytical methods for specification testing in lot release.

Small-molecule conjugation to mAbs, using any type of strategy, has enormous potential to produce several

Figure 1: ADC structures showing different sites of attachment to mAb of the drug with the linker. MMAE = monomethyl auristatin E, an extremely potent synthetic antineoplastic agent.

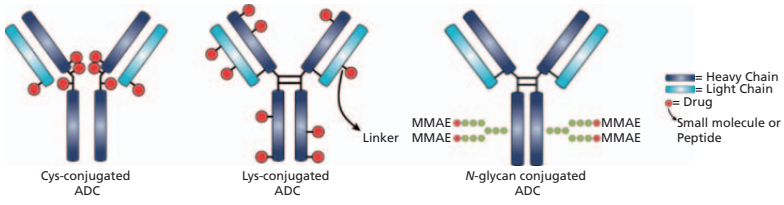

Figure 2: Typical characterization approaches performed on ADC therapeutics.

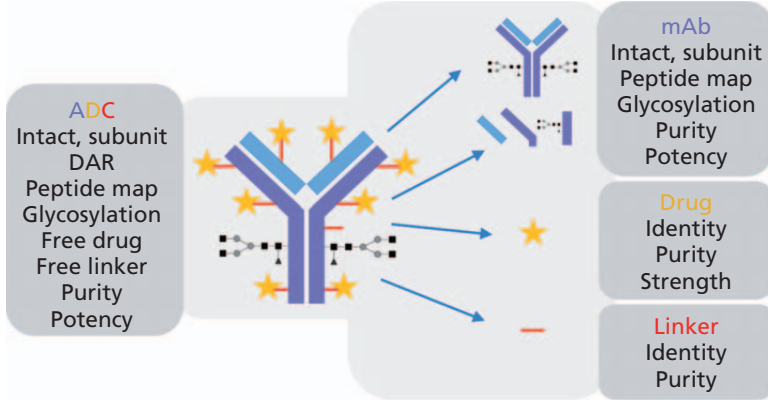

variant isoforms. Appropriate tests are needed to measure heterogeneity and ensure product consistency. Routine QC testing and characterization may measure the following characteristics:

- Aggregates and fragments
- Charge variants
- Free drug
- Average drug-to-antibody ratio (DAR)
- Drug load distribution, including unconjugated mAb
- Endotoxins or bioburden

Because of the heterogeneity of ADCs, isoforms derived from mAb glycosylation and other post-translational modifications (PTMs) are often controlled at the point of mAb release. The inclusion in the certificate of analysis (CoA) for routine testing of other product-related impurities—such as aggregates, fragments, charge variants, and unconjugated antibodies—discussed above should be assessed product by product. For example, data could be generated to show that an unconjugated antibody is adequately monitored and controlled as part of DAR testing.

Chemical impurities other than free drug or drug-related substances may be evaluated with both ICH Q3B (R2) limits and pharmacology or toxicology input for the specific product (14). Some process-related impurities might be omitted from release testing with sufficient data and process experience over multiple ADC lots or multiple ADC products using the same conjugation platform.

Regulators consider compendial monographs, which exist for small-molecule intermediates, to be the minimum standard for chemical components when used in ADCs.

Drug and Linker: Approaches and Chemistries

The conjugation of anticancer payloads to lysine or cysteine residues found in mAbs results in the generation of ADCs that exhibit significant heterogeneity, with some of the ADC potentially having altered antigen-binding properties leading to suboptimal potency, solubility, stability, and pharmacokinetics. To reduce heterogeneity, expand payload options, and prolong circulating stability, novel site-specific conjugation approaches are actively being pursued within the field (15).

The hydrophobic nature of the payloads used in current ADCs leads to the creation of conjugates of increasing hydrophobicity versus their starting mAb scaffolds. The hydrophobicity of ADCs can promote aggregation, which in turn can lead to hepatotoxicity (16) or increased immunogenicity (17). The hydrophobicity of ADCs can also promote drug resistance via increased affinity for multidrug resistance transports, with the incorporation of hydrophilic linker chemistries shown to bypass multidrug resistance (18).

ADCs use three main tumour-specific microenvironmental factors to selectively release their cytotoxic payloads: cleavable linkers exhibiting protease-sensitivity, pH-sensitivity, and glutathione-sensitivity. Within each of these main linker release mechanisms, significant linker technology advancements are ongoing.

Among the types of conjugation chemistries, enzyme-based site-specific modification shows great potential by eliminating the potential interruption of an antibody–antigen interaction and providing a highly reproducible and modular conjugation system when compared to standard lysine and cysteine conjugation.

Developments in linker chemistries also provide a greater opportunity to incorporate increasingly potent cytotoxic payloads. Quaternary ammonium linkers now enable stable conjugation of payloads with tertiary amine residues (19); the extremely potent synthetic antineoplastic agent monomethyl auristatin E (MMAE) has been linked to mAbs via a linker that is selectively cleaved by cathepsin (for example, in Adcetris) upon entrance into the tumour cell (20). A conjugate with the potent maytansinoid DM1 has been approved (for example, Kadcyla), and Seattle Genetics recently published work on a novel methylene alkoxy carbamate (MAC) self-immolative unit for hydroxyl-containing payloads within ADCs (21). The latter compound enables direct conjugation of drugs through alcohol functional groups that are present on a diverse range of synthetic drugs as well as natural cytotoxic products. Most

F-DGSi
Innovative Gas System Company

N2 GAS GENERATOR

Suitable for all OEM' S LCMS Analyzers on the Market !

REDUCE THE STRESS OF CHANGE OVER WITH A

- Proven
- Concenient
- Intelligent
- Safe

F-DGSi GAS GENERATOR

KEY FEATURES

- N2 flow rate : 15, 25, 35, 40, 64 L/min
- N2/AIR available
- Proven PSA and Membrane technology
- Built in with oil free air compressor in option
- Touch screen control with Remote access software

WWW.F-DGS.COM

Figure 3: Trastuzumab emtansine lysine-conjugation mapping (26). (a) Colour-coded base peak ion chromatogram (BPI) showing heavy and light chain peptides. (b) Coverage map showing 100% sequence coverage, number of MS peaks, and relative abundance of heavy and light chain peptides detected. (c) Example higher energy collisional dissociation (HCD) MS/MS spectrum of a glycopeptide showing fragmentation of both peptide and glycan. (d) Identification of lysine conjugated MCC-DM1 at the peptide level.

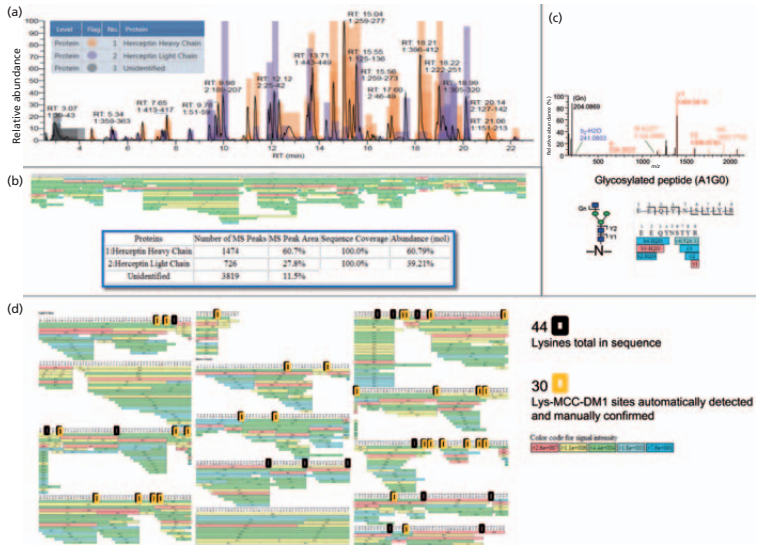

Figure 4: Comparison of synthesized Cys-conjugated ADC mimics with different drug load (29): (a) unconjugated mAb (5 mg/mL), (b) Cys-conjugated ADC mimic (low load, 5 mg/mL), (c) Cys-conjugated ADC mimic (moderate load, 5 mg/mL), (d) Cys-conjugated ADC mimic (high load, 5 mg/mL). Column: 100 mm × 4.6 mm, 5-µm d_p Thermo Scientific MAbPac HIC-Butyl; mobile-phase A: 95:5 (*v/v*) 1.5 M ammonium phosphate (pH 7.0)–isopropanol; mobile-phase B: 80:20 (*v/v*) 50 mM sodium phosphate (pH 7.0)–isopropanol; gradient: 0% B for 6 min, 0–100% B in 14 min, hold at 100% B for 5 min; temperature: 25 °C; flow rate: 1.0 mL/min; injection volume: 5 µL (5 mg/mL); detection: UV absorbance at 280 nm.

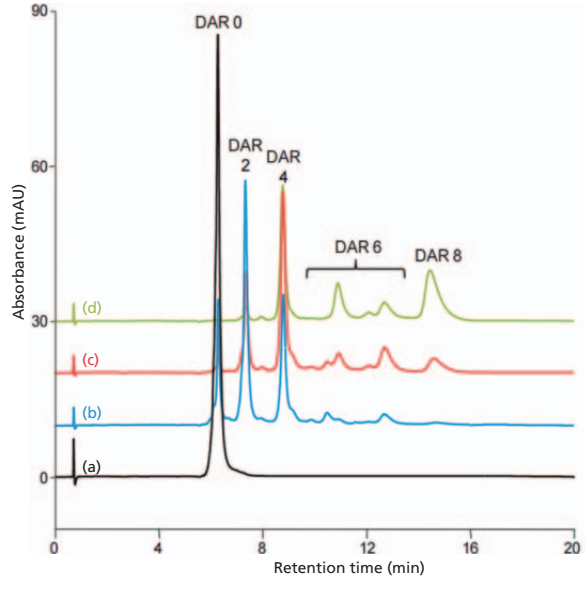

recently, Spirogen (now part of the AstraZeneca Group) developed a potent and flexible class of ADC payload based on a proprietary pyrrolobenzodiazepine (PBD) technology. PBDs are a family of sequence-selective DNA minor-groove binding agents and are among the most cytotoxic agents known. They are ideally suited for antibody–drug conjugation because of their unique mechanism of action that retains activity against cancer stem cells and is compatible with multiple linker and conjugation technologies. There are two ADCs currently undergoing clinical trial from the collaborative efforts of Spirogen and Seattle Genetics (22), and many more are in the pipeline. As previously mentioned, most of the payload and linker technologies used or studied today impart increasing levels of hydrophobicity on the mAb scaffold (10); for example, DM1 has an estimated LogP value of 3.95 per molecule incorporated. PBDs are even more hydrophobic, with an estimated LogP value of 5.08 per incorporated molecule. To address this issue, hydrophilic spacers (for example, para-aminobenzyl alcohol [PAB]) and linkers (such as polyethylene glycol [PEG]) are often incorporated as part of the bioconjugation chemistry to balance out the increased hydrophobicity introduced by the conjugation of the payload.

Chromatography for mAb, Drug, Linker, and ADC

Various ultrahigh-pressure liquid chromatography (UHPLC) techniques have proved to be useful for analyzing ADC heterogeneity at the intact level, including hydrophobic-interaction chromatography (HIC), ion-exchange chromatography (IEC), size-exclusion chromatography (SEC), and reversed-phase chromatography. Where appropriate, the coupling of these separation techniques with high-resolution accurate mass spectrometry (HRAM MS) presents a powerful characterization tool. Further structural details can be ascertained by breaking down the intact ADC; both peptide mapping using reversed-phase chromatography and released glycan analysis with hydrophilic-interaction chromatography (HILIC) are deemed essential tools. Each of these analytical approaches reveals different CQAs of the ADC—from primary amino acid sequence and associated modifications (peptide mapping) to the presence of higher order aggregated structures (SEC) that could impact product efficacy and safety. In addition to the standard cohort of small molecule and

FREE

CHROMACADEMY MEMBERSHIP

Agilent Technologies is offering five years complimentary access to CHROMacademy for all university students and staff.

CHROMacademy is an intuitive, comprehensive e-learning and trouble-shooting platform with more than 3,000 pages of content for HPLC, GC, sample preparation, and hyphenated techniques. No other online resource offers separation scientists more live streaming events, a knowledge base, practical solutions, and new technologies in one easy to navigate website.

Get your free five year membership worth US $1,995* by submitting the form at **www.chromacademy.com/agilent**.

* Five years free access to CHROMacademy only available to customers affiliated with an academic or research institution, conditions apply. A valid university e-mail address if required.

Agilent Technologies

Figure 5: Charge variant chromatographic profile comparison of commercial chimeric IgG1 mAb (black trace) and cetuximab biosimilar candidate (blue trace) obtained with cation-exchange chromatography in pH-based gradient mode (31). Peak labelling corresponds to the number of peaks in each trace and does not indicate peak identification.

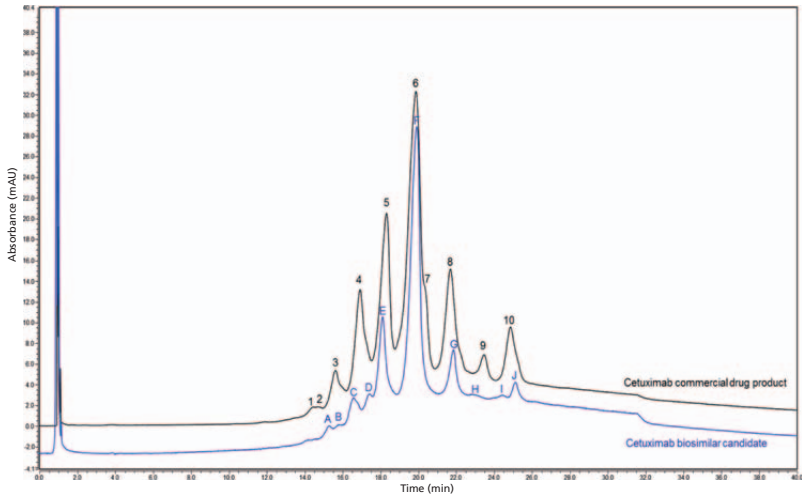

Figure 6: Denaturing LC–MS analysis of the ADC brentuximab vedotin (Adcetris) (33). (a) Unmodified sample (1 µg) was analyzed by reversed-phase chromatography coupled to an orbital trap MS system produced several peaks. (b) The resulting averaged MS spectrum is a complex mixture of charge state envelopes as well as a vcMMAE-specific reporter fragment ion at *m/z* 718. (c) Data analysis with ReSpect deconvolution and Sliding Window integration show roughly six covalently-structured forms of unraveled cysteine-linked ADC.

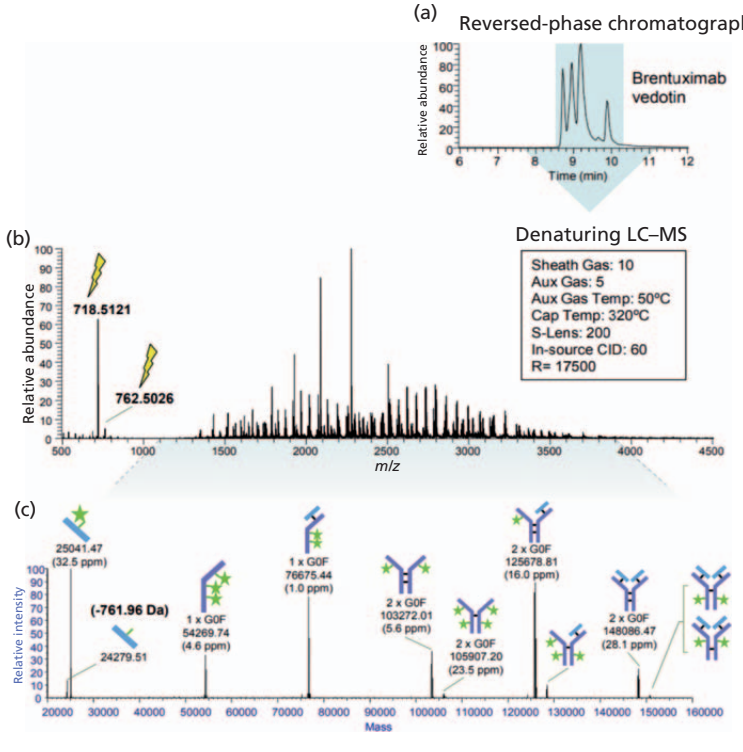

large biomolecule characterization methodologies, a whole set of tests must be performed to interrogate the level of drug conjugation and the levels of unconjugated mAb, payload, and linker (as shown in Figure 2).

Monoclonal Antibody Primary Sequence Analysis

As a technique, peptide mapping is well established in the biotechnology industry with roots lying in protein characterization, proteomics, and de novo peptide sequencing. In recent years, advances in sample preparation (protein digestion), peptide separation, HRAM MS capabilities, and bioinformatics have enabled the biotech industry to confidently apply peptide mapping workflows in routine, high-throughput environments.

Peptide mapping can reveal many CQAs of a protein. In the case of ADCs, peptide mapping is fundamental in confirming not only the sequence of the mAb, but also the site and level of drug conjugation (Figure 3). The accuracy with which this information can be determined is based on the method of protein digestion and fidelity of the subsequent UHPLC and MS analysis. The type of fragmentation used within the MS system should also be carefully considered because standard collision-induced dissociation (CID) experiments often fail to reveal the precise site of drug conjugation or glycosylation. Alternative or additive fragmentation techniques such as higher energy collisional dissociation (HCD), electron transfer dissociation (ETD), and ultraviolet photodissociation (UVPD) are becoming increasingly important in the elucidation of site-specific modifications and can generate informative fragmentation patterns, even at the subunit level (23–25).

Chromatographic Techniques for the Determination of Antibody Variants, Fragments, DAR, and Payload Mapping

Hydrophobic Interaction

Chromatography: HIC separates proteins by the interactions between hydrophobic pockets present on the surface of the protein and the hydrophobic ligands on the HIC resin. Proteins are loaded onto the column in relatively high salt concentrations to induce hydrophobic interactions and are eluted by reducing the salt concentration of the mobile phase during the chromatographic separation. The binding of the proteins is dependent on the inherent surface hydrophobicity, which is influenced by the conformation of the protein.

Changes in protein conformation can be characterized by this mode of chromatography, and several publications exist that indicate that common modifications of mAbs, such as oxidation and deamidation, can be seen using HIC (27). With the conjugation of hydrophobic payloads to the mAb to form ADCs, the use of HIC for DAR analysis has become increasingly popular (6,28).

With each additional linkage of the drug to the mAb the retention of the ADC species on the column increases, thus allowing quantification of drug load on the ADC and resolution of isomeric configurations of the same DAR (Figure 4).

Ion-Exchange Chromatography: IEC involving cation-exchange column chemistries is a standard method used to separate and monitor the charge-variant profile of mAb-based therapeutics (30). Charge-variant separations have been further developed with the use of pH gradients that provide ease of use and a more global approach to the method development process (Figure 5) (31). There are several PTMs that can alter the charge or conformation of a protein and can, therefore, be characterized using IEC. Glycan variants, deamidation, oxidation, and even aggregation are among them. The specific charge-variant profile that is obtained from a mAb is closely monitored at each stage in the production to ensure the product quality remains the same. In the case of ADCs, mAbs may not provide an informative charge-variant profile—if the drug or linker is charged, or linkage occurs through a charged amino acid (such as lysine), the underlying mAb charge heterogeneity is difficult to assess because conjugation affects the overall charge of the conjugated molecule. In such cases, the "charge profile" is often more of a "conjugation profile". Despite this, measuring the distribution of charged species can be a good way to demonstrate process consistency and thus should be included in an ADC comparability toolkit.

Reversed-Phase Chromatography-MS: MS analysis of ADC drug distribution provides insights into the relative concentration of different drug-linked forms, which may elicit distinct pharmacokinetic and toxicological properties. MS analysis of ADC drug distribution is particularly advantageous for conjugates produced using linkage through surface-accessible lysine residues, which are not easily separated by chromatography alone because of their high degree of heterogeneity.

Reversed-phase LC–MS can be used to elucidate the positional isomers of ADCs. Reversed-phase LC–MS following IdeS proteolytic digestion facilitates the subunit analysis of ADCs and enables rapid comparison of the ADC samples, for instance for batch assessment (Figure 6). Indeed, IdeS proteolytic digestion has been proposed as an analytical reference method at all stages of ADC discovery, preclinical and clinical development, for routine comparability assays, formulation, process scaleup and transfer, and to define CQAs in a QbD approach (32).

Chromatography and Native Mass Spectrometry: The ADCs currently

Figure 7: Desalting SEC-MS DAR of Adcetris and Kadcyla (35). (a) Desalting SEC is compatible with a native MS approach and allows preservation of noncovalent interactions which support the structure of cysteine-linked ADCs. Based on the individual deconvoluted abundances of the G0F/G0F glycoform, the authors calculated an average DAR value of 4.07 (32). (b) Denaturing MS spectra (from reversed-phase LC) are observed at lower *m/z* ranges while native MS spectra from online SEC are observed at higher *m/z* ranges. A detailed view shows that 2–3 sequential charge state envelopes overlap compared to an overlap of 0–1 charge state envelopes in the native MS spectrum.

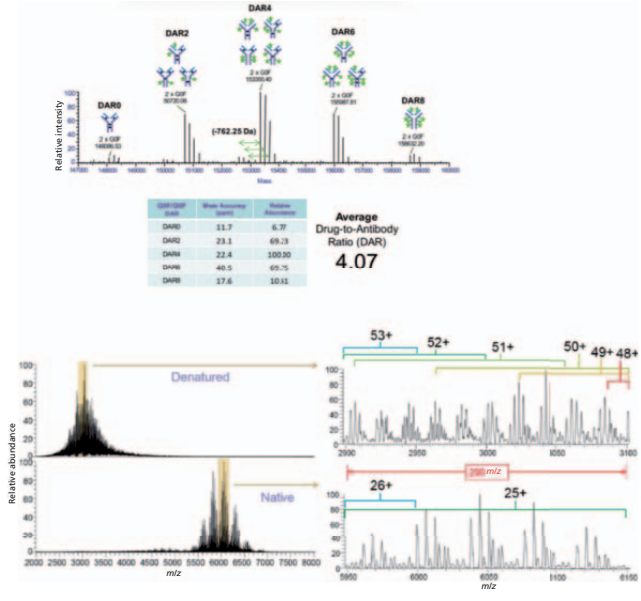

approved for use utilize naturally occurring lysine side chain amino groups or the cysteine thiol groups, which are formed upon partial reduction of IgG intramolecular disulfide bonds, for conjugation of the drug load (34).

Cysteine-linked ADCs present a unique challenge for characterization because proper intact analysis requires native MS conditions to preserve structurally critical noncovalent binding between antibody chains.

ADCs exhibit significant heterogeneity resulting from the number and distribution of drug molecules across the antibody. This level of molecular complexity and heterogeneity presents a considerable challenge for current analytical techniques.

Native MS of intact proteins allows direct observation of molecules that rely on noncovalent interactions to preserve critical structural features, such as interchain associations that hold together cysteine-linked ADCs. The use of 100% aqueous and physiological pH buffers in native MS analysis produces decreased charge states (increased *m/z*) and improves mass separation of heterogeneous mixtures.

An orbital trap native MS workflow has recently been developed that is compatible with SEC, allowing online desalting and sample delivery, to observe intact proteins at high *m/z* ranges. This strategy reduces mass interference in complex protein spectra by increasing peak capacity in the *m/z* space. This workflow has recently been applied to the analysis of Adcetris and Kadcyla, cysteine-linked and lysine-linked ADCs, respectively, and the accurate calculation of DAR (Figure 7).

This work built on a similar approach that was first applied to the study of Adcetris using an orbital trap mass spectrometer equipped with a high-mass quadrupole mass selector (36).

Higher Order Structural Analysis

Hydrogen–deuterium exchange (HDX)-MS is a powerful tool for studying the dynamics of higher-order structure of protein-based therapeutics. The rate of hydrogen-to-deuterium exchange within the amide hydrogen on the backbone of biotherapeutics provides solvent accessibility information, and thus protein structure and conformation can be inferred.

Although HDX-MS cannot be used to define an absolute structure in the manner of X-ray crystallography, it can be used to directly assess the native structure in a comparative fashion. Proteins in solution are highly dynamic, and the stability and functionality of any protein therapeutic are closely associated to a specific conformation.

The manufacturing of ADCs involves additional processing steps during conjugation, and it is important to evaluate how the drug conjugation process impacts the conformation and dynamics of the mAb intermediate. The ability of HDX-MS to monitor conformational changes at the peptide level makes the technique well-suited for providing detailed insights into the impact of drug conjugation processes on the higher-order structure of mAbs.

Orbital trap–based HDX-MS has previously been used to probe the conformation and dynamics of interchain cysteine-linked ADCs (37). In this publication, a side-by-side HDX comparison of ADCs, mAbs, reduced mAbs, and partially reduced mAbs was used to identify minor local conformational changes and confirm that these were because of the partial loss of interchain disulfide bonds in ADCs. These findings were used to indicate that ADC manufacturing processes that involve partial reduction of mAb interchain cysteine residues followed by conjugation with drug linkers do not significantly impact the conformational integrity of the mAb. A similar approach has been used to study the antibody structural integrity of site-specific ADCs (38). Together these results highlight the utility of HDX-MS for interrogating the higher-order structure of ADCs and other protein therapeutics.

Residual Free Drug Analysis and Control Strategy for Small Molecule Impurities in ADCs

Because the payload in an ADC is highly toxic, the amount of residual free drug and its impurities are CQAs. ADCs are an emerging class of biopharmaceuticals, and there are no specific guidelines addressing impurity limits and qualification requirements. Furthermore, small molecule impurities can be categorized as conjugatable impurities that could be bound to the ADC or nonconjugatable impurities that are likely to be purged during the

Table 1: Impurity dose based on the level of conjugatable impurities in the linker-drug intermediate (table adapted with permission from reference 39)

Impurity Level in Linker-Drug	Maximum Impurity Level in DS (wt/wt%)	ADC 5 mg Dose		ADC 50 mg Dose		ADC 50 mg Dose	
		Maximum Impurity Level	Maximum Daily Impurity Level	Maximum Impurity Level	Maximum Daily Impurity Level	Maximum Impurity Level	Maximum Daily Impurity Level
3%	1.5 µg/mg DS (0.15%)	7.5 µg/dose	0.36 µg/day	75 µg/dose	3.6 µg/day	0.75 mg/dose	36.0 µg/day
1%	0.5 µg/mg DS (0.05%)	2.5 µg/dose	0.1 µg/day	25 µg/dose	1.2 µg/day	0.25 mg/dose	12.0 µg/day
0.5%	0.25 µg/mg DS (0.025%)	1.25 µg/dose	0.06 µg/day	12.5 µg/dose	0.6 µg/day	0.125 mg/dose	6.0 µg/day
0.1%	0.05 µg/mg DS (0.005%)	0.25 µg/dose	0.01 µg/day	2.5 µg/dose	0.12 µg/day	0.025 mg/dose	1.2 µg/day

manufacturing process. Gong and colleagues published a white paper on a control strategy for small-molecule impurities in ADCs (39) as a working group member of the International Consortium for Innovation and Quality in Pharmaceutical Development (IQ). The strategy suggested a science- and risk-based approach predicated on the ICH Q3A (40), Q3B (14), Q5B (41), and M7 (42) (genotoxic impurities) guidelines, and include the conjugation potential of the small molecule impurities, typical dosing concentration and schedule, and their levels in the linker-drug intermediate. The control of conjugatable impurities is best achieved at the stage of manufacturing the linker-drug intermediate rather than at the drug substance or drug product while nonconjugated impurities, including free drugs, are generally cleared effectively by typical manufacturing processes. Table 1 shows the IQ recommendations of the maximum allowable dose based on these considerations.

On the analytical front, one approach to conducting free-drug analysis for ADC drug substance and drug-product preparations is to precipitate the proteins (along with protein-bound drug) and analyze the resulting supernatant using a method that is effective for detecting the small molecule such as those using UHPLC–MS or UHPLC with ultraviolet (UV) detection.

Residual Solvents and Volatile Organic Impurities in ADCs

It is uncommon that residual solvent analysis is conducted for post-production quality assurance of conventional protein-based biopharmaceuticals such as mAbs. Organic solvents are not typically used in cultured cell trains and seldom form part of the risk profile of the drug.

In contrast, the conjugation reaction to form ADCs generally involves a site-selective enzymatic or chemical reaction of antibody to linker to small-molecule drug warhead, where the hydrophobic warhead and linker are solubilized in solvents such as *N,N*-dimethylacetamide (DMA), *N,N*-dimethylformamide (DMF), dimethyl sulfoxide (DMSO), or propylene glycol (PG). The conjugation process is followed by protein purification techniques to remove process-related contaminants (unconjugated toxin and residual solvents). However, strategies must be in place to monitor for such impurities. For the analysis of these residual solvents, one possible approach is to use a direct gas chromatography (GC) technique (43) after removal of the proteins rather than the traditional headspace GC approach in *USP* <467> (44). Because of the low levels expected for residual solvents in ADC samples, an alternative GC–MS method (particularly using the selected ion monitoring mode) is likely to yield higher sensitivity as well as provide identification information on unknown peaks, as shown in the example in Figure 8.

Figure 8: GC–MS of residual solvents following analytical headspace GC conditions similar to those in *USP* <467> that may provide higher sensitivity under single ion monitoring mode as well as information for unknown peak identification.

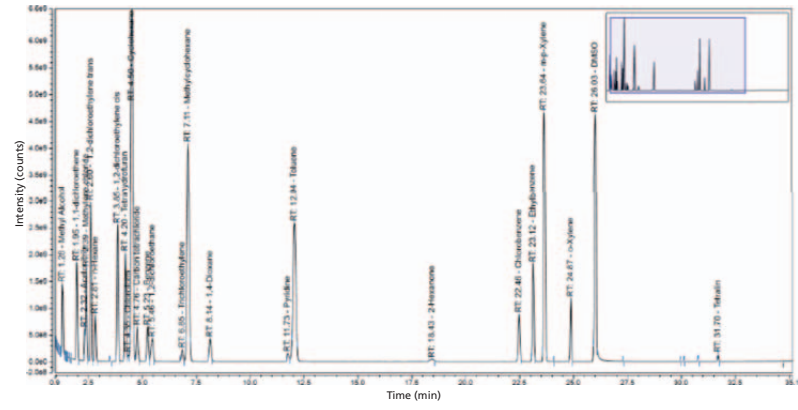

Bioanalysis of ADCs

ADCs are complex heterogeneous mixtures resulting from differences

in glycosylation of the antibody, the number of small-molecule drug moieties attached to the antibody, and the location of the conjugation sites. This situation is further complicated as the drug undergoes *in vivo* changes such as spontaneous deconjugation of the small-molecule drug and differential clearance rates of ADC components as a result of their different DARs. These changes, as well as other attributes of ADCs, contribute to the unique challenges in their bioanalysis. Furthermore, it is becoming clearer that the data required by the bioanalytical scientist is also dependent on the phase of the ADC development. The early discovery phase requires *in vivo* stability of ADC candidates based on monitoring average DAR or presence and integrity of the drug moiety at a specific conjugation site, while in the clinical development phase, it is important to establish a correlative relationship between one or more components of the ADC and various safety and efficacy indicators. Therefore, to address these bioanalytical challenges both ligand binding assays (LBAs) and LC–MS have been used. For instance, measurement of total antibody to assess antibody pharmacokinetic (PK) behaviour and measurement of conjugated antibody (DAR $\geq$ 1) is typically performed using LBAs, with unconjugated drug monitored by LC–MS. However, a hybrid of the two approaches, referred to as *hybrid LC–MS*, is becoming more actively developed and applied in ADC bioanalysis. This platform uses the affinity capture of the LBA to retain sensitivity and LC–MS for detection to provide greater specificity and improved characterization of the ADC component being monitored. Therefore, the hybrid LC–MS approach provides benefits of both the LBA and LC–MS, enabling scientists to better address some of the unique challenges of ADC bioanalysis and to allow for the use of a single platform to generate the data required for ADC bioanalysis (45).

Summary

ADCs are an increasingly important class of biotherapeutics. As the list of the first-generation ADCs entering the clinic grows, new generations of ADCs will benefit from their insights. The future looks set to see ADCs that have higher levels of cytotoxic drug conjugation, lower levels of unconjugated antibodies, more-stable linkers between the drug and the antibody, and increasing analytical challenges. The stability of linkers in circulation is critical to ensure patient safety and to mitigate the side effects caused by the off-target release of toxic payloads.

Today's ADCs pose unique analytical challenges requiring increasingly powerful approaches, consisting of small- and large-molecule techniques for their comprehensive characterization. The complexity of their analysis is matched only with their potential to become the "magic bullet" of anticancer treatment.

Acknowledgements

The authors thank Davy Guillarme and Szabolcs Fekete of the University of Geneva, Michael Heidorn of Thermo Fisher Scientific, Tao Chen and Chris Yu of Genentech, Francois D'Hooge of Novasep, He Meng of Sanofi, Srikanth Kotapati of BMS, and Yanqun Zhao of AbbVie for providing technical and editorial inputs to the manuscript.

References

(1) *Antibody-Drug Conjugates: Fundamentals, Drug Development, and Clinical Outcomes to Target Cancer*, K.J. Olivier and S.A. Hurvitz, Eds. (Wiley, Hoboken, New Jersey, USA, 2017), pp. 1–560.

(2) *Antibody-Drug Conjugates: The 21st Century Magic Bullets for Cancer*, J. Wang, W-C. Shen, and J. L. Zaro, Eds. (AAPS Advances in the Pharmaceutical Sciences Series, Springer, Heidelberg, Germany, 2015).

(3) N. Diamantis and U. Banerji, *Br. J. Cancer* **114**(4), 362–367 (2016).

(4) H.J. Wang, T. Zhang, B.J. Agnew, R. Viner, S. Lin, S. Houel, and J. Josephs, "Orbitrap Based Mass Spectrometric Characterization of Antibody Drug Conjugates Engineered through Antibody Glycans," Thermo Scientific Poster Note, accessed online January 2018 (https://tools.thermofisher.com/content/sfs/posters/PN-64397-LC-MS-ADC-Antibody-Glycans-AAPS2015-PN64397-EN.pdf).

(5) R.S. Zolot, S. Basu, and R.P. Million, *Nat. Rev. Drug Discovery* **12**, 259–260 (2013).

(6) A. Wakankar, Y. Chen, Y. Gokarn, and F.S. Jacobson, *MAbs* **3**, 161–172 (2011).

(7) A. Beck, L. Goetsch, C. Dumontet, and N. Corvaïa, *Nat. Rev. Drug Discovery* **16**(5), 315–337 (2017).

(8) B. Bobály, S. Fleury-Souverain, A. Beck, J.L. Veuthey, D. Guillarme, and S. Fekete, *J. Pharm. Biomed. Anal.* **147**, 493–505 (2018).

(9) T. Chen, Y. Chen, C. Stella, C.D. Medley, J.A. Gruenhagen, and K. Zhang, *J. Chromatogr. B* **1032**, 39–50 (2016).

(10) R. Neupane and J. Bergquist, *Eur. J. Mass Spectrom.* **23**(6), 417–426 (2017).

(11) International Conference on Harmonization, *ICH Harmonised Tripartite Guideline, ICH Q6A Specifications: Test Procedures and Acceptance Criteria for New Drug Substances and New Drug Products: Chemical Substances* (ICH, Geneva, Switzerland, 2000).

(12) International Conference on Harmonization, *ICH Harmonised Tripartite Guideline, ICH Q6B: Specifications: Test Procedures and Acceptance Criteria for Biotechnological/Biological Products* (ICH, Geneva, Switzerland, 1999).

(13) SigmaMAb Antibody-Drug Conjugate (ADC) Mimic product webpage, Sigma-Aldrich, United Kingdom, accessed online January 2018 (https://www.sigmaaldrich.com/catalog/product/sigma/msqc8?lang=en&region=GB).

(14) International Conference on Harmonization, *ICH Harmonised Tripartite Guideline: Impurities in New Drug Products, ICH Q3B (R2)* (ICH, Geneva, Switzerland, 2006).

(15) J.R. McCombs and S.C. Owen, *AAPS J.* **17**(2), 339–351 (2015).

(16) L.M. Jarvis, *Chem. Eng. News* **90**(25), 12–18 (2012).

(17) M.K. Joubert, M. Hokom, C. Eakin, L. Zhou, M. Despande, M.P. Baker, *et al.*, *J. Biol. Chem.* **287**(30), 25266–25279 (2012).

(18) Y.V. Kovtun, C.A. Audette, M.F. Mayo, G.E. Jones, H. Doherty, E.K. Maloney, *et al.*, *Cancer Res.* **70**, 2528–2537 (2010).

(19) P.J. Burke, J.Z. Hamilton, T.A. Pires, J.R. Setter, J.H. Hunter, J.H. Cochran, A.B. Waight, and K.A. Gordon, *Mol. Cancer Ther.* **15**(5), 938–945 (2016).

(20) J.A. Francisco *et al.*, *Blood.* **102**(4), 1458–1465 (2003).

(21) R.V. Kolakowski, K.T. Haelsig, K.K. Emmerton, C.I. Leiske, J.B. Miyamoto, J.H. Cochran, R.P. Lyon, P.D. Senter, and S.C. Jeffrey, *Angew Chem. Int. Ed. Engl.* **55**(28), 7948–7951 (2016).

(22) J. Mantaj, P.J.M. Jackson, K.M. Rahman, and D.E. Thurston, *Angew Chem. Int. Ed. Engl.* **56**(2), 462–488 (2017).

(23) J. Qian and M. Sanders, "Degradation Profiling of a Monoclonal Antibody Using Multiple Fragmentation Techniques and a Novel Peptide Mapping Software," Thermo Fisher Scientific Poster Note, Accessed online October 2017 (https://tools.thermofisher.com/content/sfs/posters/PN-64146-Degradation-Profiling-ASMS2014-PN64146-EN.pdf).

(24) J.S. Brodbelt, *Chem. Soc. Rev.* **43**(8), 2757–2783 (2014).

(25) S. Lu, S.-B. Fan, B. Yang, Y.-X. Li, J.-M. Meng, L. Wu, P. Li, K. Zhang, M.-J. Zhang, Y. Fu, J. Luo, R.-X. Sun, S.-M. He and M.-Q. Dong, *Nat. Methods* **12**, 329–331 (2015).

(26) A.O. Bailey, S. Houel, E. Damoc, K. Scheffler, and J.L. Josephs, "Integrated Characterization of a Lysine-Linked Antibody-Drug Conjugate by Native Intact Mass Analysis and Peptide Mapping Performed on a Hybrid Quadrupole-Orbitrap Mass Spectrometer with High Mass Range," Thermo Scientific Poster Note, accessed online January 2018. (https://tools.thermofisher.com/content/sfs/posters/PO-72282-LC-MS-Lysine-Linked-ADCs-ATE2017-PO72282-EN.pdf)

(27) J.V. Douglass, A. Wallace, and A. Balland, *J. Chromatogr. A* **1214**(1–2), 81–89 (2008).

(28) A. Cusumano, D. Guillarme, A. Beck, and S. Fekete, *J. Pharm. Biomed. Anal.* **121**, 161–173 (2016).

(29) J. Baek, I. Birznieks, S. Lin, and X. Liu, "Analysis of Monoclonal Antibodies and Antibody-Drug Conjugates Using New Hydrophobic Interaction Chromatography (HIC) Columns," Thermo Scientific Poster Note, accessed online January 2018 (https://tools.thermofisher.com/content/sfs/posters/PN-21218-HPLC-Monoclonal-Antibodies-HIC-PN21218-EN-Rev1.pdf).
(30) M. Weitzhandler, D. Farnan, J. Horvath, J.S. Rohrer, R.W. Slingsby, N. Avdalovic, and C. Pohl, *J. Chromatogr. A* **828**(1–2), 365–372 (1998).
(31) S. Millán, A. Trappe, A. Farrell, and J. Bones, "Simple Charge Variant Profile Comparison of an Innovator Monoclonal Antibody and a Biosimilar Candidate," Thermo Scientific Application Note (in press, 2018).
(32) E. Wagner-Rousset, M.-C. Janin-Bussat, O. Colas, M. Excoffier, D. Ayoub, J.-F. Haeuw, I. Rilatt, M. Perez, N. Corvaïa, and A. Beck, *MAbs* **6**(1), 173–184 (2014).
(33) "Cysteine Linked Antibody-Drug Conjugate Performed on a Hybrid Quadrupole-Orbitrap Mass Spectrometer with High Mass Range," Thermo Scientific Poster Note, accessed online January 2018 (https://assets.thermofisher.com/TFS-Assets/CMD/posters/PN-64802-LC-MS-Cysteine-linked-Antibody-Drug-Conjugate-ASMS2016-PN64802-EN.pdf).
(34) A. Beck, J.-F. Haeuw, T. Wurch, L. Goetsch, C. Bailly, and N. Corvaïa, *Discovery Med.* **10**(53), 329–339 (2010).
(35) A.O. Bailey, S. Houel, K. Scheffler, E. Damoc, J. Sutton, and J. L. Josephs, "Complete Characterization of a Lysine-Linked Antibody-Drug Conjugate by Native LC/MS Intact Mass Analysis and Peptide Mapping," Thermo Scientific Application Note, accessed online January 2018 (https://assets.thermofisher.com/TFS-Assets/CMD/Application-Notes/an-72511-lc-ms-lysine-linked-adc-an72511-en.pdf).
(36) A. Dyachenko, G. Wang, M. Belov, A. Makarov, R.N. de Jong, E.T. van den Bremer, P.W. Parren, and A.J. Heck, *Anal. Chem.* **87**(12), 6095–6102 (2015).
(37) L.Y. Pan, O. Salas-Solano, and J.F. Valliere-Douglass, *Anal. Chem.* **86**(5), 2657–2664 (2014).
(38) L.Y. Pan, O. Salas-Solano, and J.F. Valliere-Douglass, *Anal. Chem.* **87**(11), 5669–5676 (2015).
(39) H.H. Gong, N. Ihle, M.T. Jones, K. Kelly, L. Kott, T. Raglione, S. Whitlock, Q. Zhang, and J. Zheng, *AAPS PharmSciTech* **19**(3), 971–977 (2018).
(40) International Conference on Harmonization, *ICH Harmonised Tripartite Guideline: Impurities in New Drug substances, Q3A (R2)* (ICH, Geneva, Switzerland, 2006).
(41) International Conference on Harmonization, *ICH Harmonised Tripartite Guideline ICH Q5B: Quality of Biotechnological Products* (ICH, Geneva, Switzerland, 1995).
(42) International Conference on Harmonization, *ICH Harmonised Guideline ICH M7(R1): Assessment and Control of DNA Reactive (Mutagenic) Impurities in Pharmaceuticals to Limit Potential Carcinogenic Risk* (ICH, Geneva, Switzerland, 2017).
(43) C.D. Medley, J. Kay, Y. Li, J. Gruenhagen, P. Yehl, and N.P. Chetwyn, *Anal. Chim. Acta* **850**, 92–96 (2014).
(44) General Chapter <467> "Residual Solvents," in *United States Pharmacopeia 40–National Formulary* **35** (United States Pharmacopeial Convention, Rockville, MD, USA). Available at: https://hmc.usp.org/sites/default/files/documents/HMC/GCs-Pdfs/c467.pdf.
(45) K. Antwi, A. Ribar, U. Kiernan, and E.E. Niederkofler, "Quantitative Analysis of an Antibody Drug Conjugate using MSIA D.A.R.T.'S Technology, an Integral Part of the Universal Ligand Binding Mass Spectrometric Immunoassay (LB-MSIA) Workflow," Thermo Scientific Application Note, accessed online January 2018 (https://assets.thermofisher.com/TFS-Assets/LCD/Application-Notes/LCD-MSIA-AnitibodyDrugConjugate-AppNote-APAACMSIAADCQuan-EN.pdf).

Rowan E. Moore PhD, MRSC, has more than 15 years of experience with LC and high resolution MS and she currently manages a Bio/Pharma applications development team at Thermo Fisher Scientific. She gained her Ph.D. from the University of Liverpool, UK, where she applied proteomic approaches to the identification and detection of pyrrolizidine alkaloidosis biomarkers in equines. Rowan has since worked in regulated bioanalysis and in roles for leading instrument manufacturers, maintaining a keen focus on the delivery of analytical solutions for customer success.

Kelly Broster PhD, is a former Cancer Research UK scientist, now focused on biopharmaceutical and pharmaceutical applications with a focus on customer needs in LC and MS at Thermo Fisher Scientific. Kelly has an M.Sc. in biomedical science, a Ph.D. in cancer proteomics, and held a postdoctoral position in systems oncology.

Ken Cook PhD, has more than 30 years of experience supporting LC and IC applications. Ken currently supports customers in bio-separations for Thermo Fisher Scientific. Previously, Ken was a lecturer in biochemistry at the University of Newcastle, UK where he focused on protein biochemistry.

Kyle D'Silva PhD, MRSC, has more than 15 years of experience in GC and HRMS, working for several instrument manufacturers. Kyle is responsible for marketing connected analytical workflow solutions for the pharmaceutical and biopharmaceutical markets at Thermo Fisher Scientific. He holds an M.Sc. in analytical chemistry and instrumentation, and a Ph.D. in research involving applied analytical chemistry and environmental sciences.

Eric Niederkofler PhD, is the R&D and Applications Manager at Thermo Fisher Scientific, currently managing activities related to the Mass Spectrometric Immunoassay (MSIA) product line. Eric has a Ph.D. in bioanalytical chemistry from Arizona State University, USA, and has authored more than 30 peer-reviewed scientific articles and book chapters on his work in the field of targeted proteomics.

Aaron O. Bailey PhD, trained in MS in the laboratory of Professor John R. Yates III at The Scripps Research Institute. He earned his doctorate in cell biology at the University of Virginia, USA, then joined Thermo Fisher Scientific as an Applications Scientist focused on large biomolecule analysis. Aaron later joined the biopharma marketing team to lead efforts in intact protein analysis, with particular focus on native MS applications.

Jonathan Bones PhD, is a Principal Investigator at the National Institute of Bioprocessing Research and Training (NIBRT). Jonathan received a Ph.D. in analytical chemistry, and then undertook postdoctoral research with Professor Pauline Rudd at NIBRT. He moved to Northeastern University in Boston, USA, working with Professor Barry L. Karger. Jonathan returned to NIBRT in 2012 following receipt of funding from Science Foundation Ireland to form his own independent research group focused on the development and application of advanced LC–MS and CE-MS solutions for the characterization and comparability assessment of therapeutic proteins and manufacturing processes.

Michael W. Dong is a principal of MWD Consulting, which provides training and consulting services in HPLC and UHPLC, method improvements, pharmaceutical analysis, and drug quality. He was formerly a Senior Scientist at Genentech, Research Fellow at Purdue Pharma, and Senior Staff Scientist at Applied Biosystems/PerkinElmer. He holds a Ph.D. in analytical chemistry from City University of New York, USA. He has more than 100 publications and a best-selling book in chromatography. He is an editorial advisory board member of *LCGC North America* and the Chinese American Chromatography Association. Direct correspondence to: LCGCedit@ubm.com

Advancing Food Analysis with Ultrahigh-Pressure Liquid Chromatography and High-Resolution Mass Spectrometry

Specialists in food analysis are increasingly interested in taking advantage of methods that harness the power of ultrahigh-pressure liquid chromatography (UHPLC) and high-resolution mass spectrometry (HRMS). Jon Wong of the Center for Food Safety and Applied Nutrition at the U.S. Food and Drug Administration has been developing such methods for a variety of types of analysis. In this interview, he talks to *LCGC* about the work to develop these methods and the advantages of their use.

Q. You collaborated in developing a method for analyzing multiple mycotoxins in finished grain and nut products using ultrahigh-pressure liquid chromatography and high-resolution mass spectrometry (UHPLC–HRMS) (1). Why did you undertake this work?

A: At the time, UHPLC–HRMS was a relatively new technology to us and it required evaluation to determine if there were significant benefits and advantages over the current and widely accepted UHPLC–triple-quadrupole MS technology (LC–MS/MS) being used for food safety analysis. We decided to focus on mycotoxins because we had recently developed an LC–MS/MS method for mycotoxins in grains and nuts (2), and since there were still materials remaining from that study, we used the same preparation procedures on the samples and analyzed them on a UHPLC–HRMS system for evaluation and comparison. UHPLC–HRMS was not only quantitative and just as sensitive as the LC–MS/MS method but it could also provide more information for identification. The results showed that the same product ions are formed in both LC–MS/MS and UHPLC–HRMS despite the different MS platforms, but the high-accuracy masses in HRMS provided better details to speculate about how the mycotoxin precursor could fragment and form into product ions. We began to realize and recognize the possibilities and the drawbacks of UHPLC–HRMS based on this experience.

Q. What are the advantages and disadvantages of UHPLC–HRMS over LC–MS/MS? For what types of analysis would you favour one technology over the other?

A: One obvious advantage of UHPLC–HRMS over LC–MS/MS is the better data quality and confidence in the results when you can determine the mass of the molecular ion to four or five decimal places. This precision is extremely useful for fragmentation studies and to assign proposed structures. An example that convinced us of one of the benefits of HRMS came from the mycotoxin studies. We were comparing and matching the mass-to-charge ratio *(m/z)* results from product ions obtained from our UHPLC–high-resolution data-dependent MS/MS experiments of ergocornine and its products with results obtained from LC–MS/MS (using a triple-quadrupole mass analyzer), provided from a publication from another research group (3). Our UHPLC–high-resolution data-dependent MS/MS results agreed with most of the results except for *m/z* 208.1. Our calculated mass of 208.07569 from our experimental results did not agree with the proposed structure 4, $C_{14}H_{12}N_2^{\bullet+}$, assigned in the other group's paper, which resulted in a calculated mass of 208.09950 but with a mass accuracy of $\delta_M = -113.05$ using the experimental mass value obtained from our HRMS studies. This result indicated to us that the proposed structure 4, shown in Figure 1, was not possible. The experimental mass indicated that the structure had to have an elemental composition of $C_{14}H_{10}NO^+$, which was possible if structure 2 were to fragment and lose $-C_2H_5N$ to form structure 5. However, we saw that the other group's paper was correct; we were able to find structure 4 at higher collision energies but we also found further evidence to support structure 5 as a loss of –CO, resulting in a calculated mass of 180.08078 to support the formation of structure 6, which was also experimentally found. These studies were extremely useful to determine the elemental composition, elucidate fragmentation patterns, and propose and assign structures of the product ions. This information can be useful and helpful by knowing the stability of these product ions and deciding the precursor-to-product ion transitions used in LC–MS/MS analysis of chemical residues and contaminants.

Photo Credit: Olha Afanasieva/Shutterstock.com

These experiences really helped us see the benefits of HRMS analysis.

LC–HRMS is still relatively new to those in the food safety and environmental field, but people are learning more about it. The main disadvantage of HRMS is that the data files are huge and eventually one needs to have sufficient storage space to save all these data.

Little prior information is required to set up an HRMS procedure with an associated full-scan component as long as the analyte can be chromatographically separated, the analyte is efficiently and effectively ionized, and the associated masses of the analyte are detected. Although LC–MS/MS is selective and sensitive, it is a restricted and targeted procedure that requires *a priori* knowledge of the analyte's retention time and precursor and product ion masses. However, LC–MS/MS is still the standard procedure for LC–MS analysis of chemical contaminants and residues. As long as you know what your target analytes are, LC–MS/MS is the preferred approach for analysis. The current identification criteria of pesticide and veterinary drug residue, natural toxins, and processing contaminants are mature and well established for LC–MS/MS analysis but they are being developed for LC–HRMS analysis.

A drawback for LC–MS/MS procedures arises in multiresidue screening, especially when the list of pesticides is large. For example, if you are screening for 500 pesticides, the MS/MS method will require at least 1000 precursor-to-product ion transitions (because two are usually required for each pesticide) and pesticide retention times. Maintaining such a method would be difficult. We are trying to develop LC–HRMS procedures to screen large volumes of compounds using HRMS/MS libraries and compound databases that may be easier to manage.

Figure 1: Fragmentation pattern of ergocornine determined using HRMS/MS.

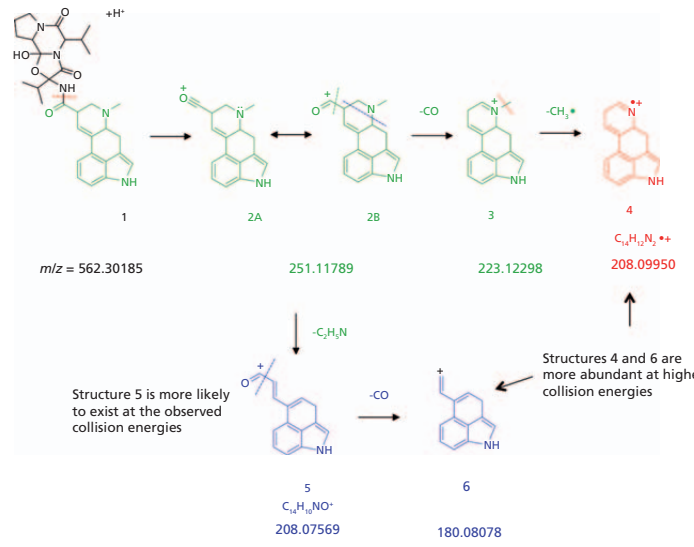

Figure 2: Schematics of (a) full-scan MS and (b) data-dependent MS/MS scan processes. Adapted with permission from reference 8.

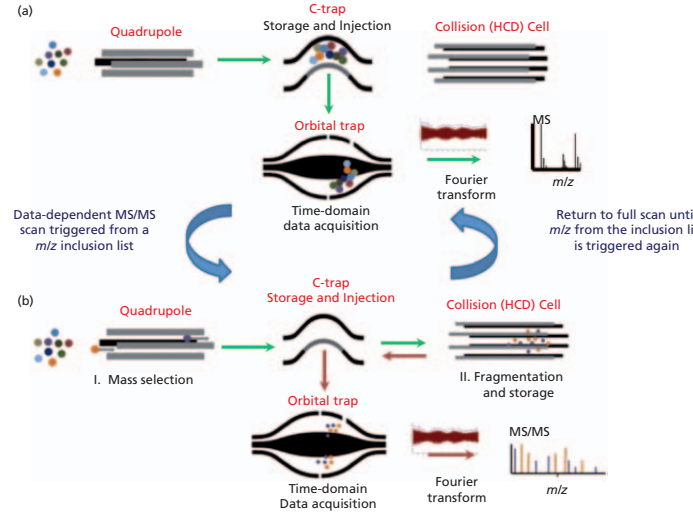

Q. Have you been able to expand the use of HRMS to the analysis of other chemicals involved in food safety?

A: Yes. We are collaborating with scientists at the Canadian Food Inspection Agency Our collaborations have led to validated UHPLC–HRMS procedures to analyze pesticides in fruits and vegetables (4) and veterinary drugs in milk (5). Typical sample preparation procedures such as QuEChERS (quick, easy, cheap, effective, rugged, and safe) for pesticides in fruits and vegetables and modifications of a procedure using solid-phase extraction for veterinary drugs on milk worked well when these extracts were analyzed with UHPLC–HRMS. In these two projects, and in the mycotoxin project, we were able to quantitatively analyze food samples using UHPLC and data-dependent acquisition HRMS (UHPLC–DDA–HRMS) and the results were obtained just as easily as with LC–MS/MS.

This work using full-scan MS and DDA MS/MS (schematic shown in Figure 2) was similar to work we had done earlier on a hybrid quadrupole–ion trap mass spectrometer to generate multiple reaction monitoring (MRM) spectra of product ions instead of the two MRM precursor-to-product transitions (6). The work on the hybrid MS system had some limitations and required scoring or matching factors that were difficult to implement for identification. The advantage of the HRMS DDA spectra is that identification could be determined based on retention time and mass accuracy of the precursor and product ions of the chemical of interest. This work and previous experiences in which using state-of-the-art technology has

Figure 3: Schematic of a full-scan data independent acquisition experiment.

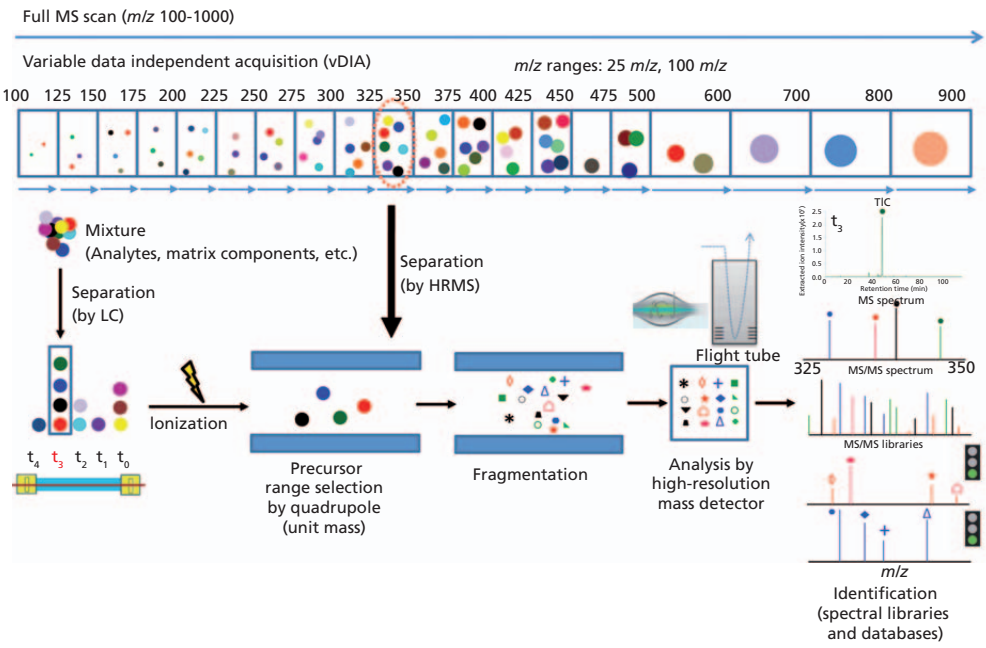

improved our work have convinced us that LC–HRMS is going to have a major role in the future of chemical residue and contaminant screening and analysis.

Q. You mentioned some of your previous collaboration with the Canadian Food Inspection Agency. More recently, you have been working with that agency to develop systematic and detailed protocols for screening for chemical residues in foods (7). Why did you start collaborating, and why did you undertake the development of this method in particular?

A: Research in developing large-scale screening methods requires a lot of resources and time, and our agencies have a mutual interest and an agreement to evaluate the UHPLC–HRMS technology and its potential applications for screening pesticides and other chemical residues and contaminants in foods. It is better to collaborate to avoid duplication of the work and to lessen the work burden since we have the same goals and interests.

We are trying to accomplish several tasks for developing effective LC–HRMS screening procedures. One is to create HRMS/MS libraries for chemical residues and contaminants such as pesticides, veterinary drugs, and mycotoxins so that we can extract the calculated masses of the product ions and deposit them into a compound database. The compound database can be implemented in the software for data processing applications such as screening, which can determine the presence of residues or contaminants that may be present in a food sample subjected to LC–HRMS analysis. The libraries and databases are tedious to build because every major product ion in the MS/MS spectra requires evaluation, but this work is necessary to build a comprehensive database. A second area we are involved in is to develop, evaluate, and validate UHPLC–HRMS/MS experiments in DDA and data-independent acquisition (DIA) modes for quantitative analysis and qualitative screening. This work has been done for the analysis of pesticides in fruits and vegetables and veterinary drugs in milk. Our goal is to determine which LC–HRMS procedure would be effective based on the application and need. Finally, by collaborating with another agency, we can perhaps harmonize what sample preparation and instrumental methods and conditions are to be used for quantitative or screening analysis for different analyte or food classes.

Q. You used the full-scan DDA mode to acquire product ion spectra of individual pesticides to obtain the accurate masses of fragments that were used to build the compound database and MS library, but you used DIA mode to acquire the sample data. Why?

A: Under DDA mode, the precursor ions are selected by the quadrupole within a narrow *m/z* window—~1–4 Da wide—and are transferred to the high energy collision dissociation (HCD) cell to produce product ions. Information of the precursor ions and their retention times are required *a priori* to trigger a targeted MS/MS response. This approach is ideal to create an MS/MS spectrum for the chemical analyte of interest because only the product ions are detected and there is minimal interference present in the spectrum due to the narrow *m/z* window. It is also ideal for building MS/MS spectra libraries. The product ions generated from the DDA-MS/MS spectra originate from only the precursor ion of interest. We initially used DDA for the quantitative analysis of mycotoxins, pesticides, and veterinary drugs because we were evaluating the HRMS using full MS and DDA-MS/MS scans to determine if we could develop a targeted approach similar to an LC–MS/MS procedure.

DIA utilizes the quadrupole to perform a precursor or survey scan of selected ions using mass range windows. In our work, a variable DIA (vDIA) procedure was developed using 16 mass range windows with a width of 25 *m/z* for

100–500 *m/z* and four mass range windows with a width of 100 *m/z* for 500–900 *m/z*. A full MS scan was also implemented from a range of 100–1000 *m/z*. The schematic of the experiment is shown in Figure 3. The ions in the vDIA experiments are subjected to fragmentation and MS/MS analysis according to the progression of the mass range window. This approach is ideal for screening applications because all of the ions in the 100–900 *m/z* range will eventually undergo fragmentation in the collision cell and the product ions will be analyzed in the mass analyzer.

The instrument software, along with the MS/MS libraries and compound databases, can be used to sort and identify any chemical present in the sample (as long as the chemical is logged in the library and database). MS/MS spectra from DIA scans for library applications are not ideal because multiple analytes can be coeluted chromatographically and can potentially be within the mass-range window. The resulting product ions would be difficult to discriminate from the different precursors in the same MS/MS spectrum. Given the smaller *m/z* window range and retention time trigger of the targeted precursor, results from DDA would be more reliable to build the library and database.

Q. What are the next steps in your work?

A: We would like to expand and apply UHPLC–HRMS to screening chemical residues and contaminants in important food commodities. It would be ideal to be able to expand and combine all the MS/MS libraries and databases to screen for not only pesticide residues but also veterinary drugs, mycotoxins, processing contaminants, and other contaminants that can potentially be present in food and other commodities. We will continue to evaluate, optimize, and advance HRMS applications to complement LC–MS/MS methods or to combine screening with quantitative analysis.

References

(1) C.-D. Liao, J.W. Wong, K. Zhang, P. Yang, J.B. Wittenberg, M.W. Trucksess, D.G. Hayward, N.S. Lee, and J.S. Chang, *J. Agric. Food Chem.* **63**, 8314–8332 (2015).

(2) C.-D. Liao, J.W. Wong, K. Zhang, D.G. Hayward, and M.W. Trucksess, *J. Agric. Food Chem.* **61**, 4771–4782 (2013).

(3) R. Mohamed, E. Gremaud, J.-C. Tabet, and P.A. Guy, *Rapid Commun. Mass Spectrom.* **20**, 2787–2799 (2006). DOI: 10.1002/rcm.2648.

(4) J. Wang, W. Chow, J. Chang, and J.W. Wong, *J. Agric. Food Chem.* **62**, 10375–10391 (2014).

(5) J. Wang, W. Chow, J. Chang, and J.W. Wong, *J. Agric. Food Chem.* **63**, 9175–9187 (2015).

(6) K. Zhang, J.W. Wong, P. Yang, D.G. Hayward, T. Sakuma, Y. Zou, A. Schreiber, C. Borton, T.V. Nguyen, K. Banerjee, and D. Oulkar, *Anal. Chem.* **84**, 5677–5684 (2012).

(7) J. Wang, W. Chow, J. Chang, and J.W. Wong, *J. Agric. Food Chem.* **65**, 473–493 (2017).

(8) A. Michalski, E. Damoc, J.P. Hauschild, O. Lange, A. Wieghaus, A. Makarov, N. Nagaraj, J. Cox, M. Mann, and S. Horning, *Mol. Cell Proteomics* **10**(9), M111.011015 (2011). DOI: 10.1074/mcp.M111.011015.

Jon W. Wong, PhD, is a research chemist at the Center for Food Safety and Applied Nutrition at the U.S. Food and Drug Administration, in College Park, Maryland, USA. Direct correspondence about this article to: Jon.Wong@fda.hhs.gov.

Bioseparation columns

Phenomenex has introduced bioZen, a new series of LC solutions for bioseparations in pharmaceutical, biopharmaceutical, and academic research. The series encompasses entirely new media spanning two particle platforms—core–shell and thermally modified fully porous—along with biocompatible titanium hardware. bioZen features seven chemistries for the UHPLC and HPLC characterization of biotherapeutics, including monoclonal antibodies, antibody–drug conjugates, and biosimilars.

www.phenomenex.com/products/detail/biozen
Phenomenex Inc. Torrance, California, USA.

LC–MS/UHPLC–MS solvents

Scharlau solvents provide the correct purity for an excellent result with simpler and cleaner spectra, according to the company. Preventing the formation of unwanted adducts with metallic impurities, longer column lifetimes, avoiding equipment blockage, and savings in equipment maintenance are reportedly the main advantages of these solvents. Each lot is checked by LC–MS or (U)HPLC–MS.

www.scharlab.com
Scharlab, S.L., Barcelona, Spain.

HILIC columns

Hilicon offers a broad range of hydrophilic interaction liquid chromatography (HILIC) products for the separation of polar compounds. Three column chemistries in UHPLC and HPLC, iHILIC-Fusion, iHILIC-Fusion(+), and iHILIC-Fusion(P), provide customized and complementary selectivity, excellent durability, and ultra-low column bleeding, according to the company. The columns are suitable for the LC–MS analysis of polar compounds in "omics" research, food and beverage analysis, pharmaceutical discovery, and clinical diagnostics.

www.hilicon.com
Hilicon AB, Umeå, Sweden.

(U)HPLC columns

YMC-Triart Bio C4 is a new wide-pore phase for (U)HPLC. As a result of its 300 Å pore size, it is designed for peptide–protein separations. The company reports it has excellent reproducibility, a high pH (1–10), and stability at temperatures up to 90 °C.

www.ymc.de
YMC Europe GmbH, Dinslaken, Germany.

GC system

Shimadzu's Nexis GC-2030 is based on the concept of excellent usability and expandability for a wide variety of analytical applications. Equipped with a full-colour LCD touch panel, it can be operated intuitively simply by touching the clearly organized and easy-to-understand interface. The system also allows users to configure various parameter settings, perform self-diagnostics, check automatically for carrier gas leaks, and display chromatograms via the interface on the main GC unit.

www.shimadzu.eu
Shimadzu Europa GmbH, Duisburg, Germany.

Mircoplate information guide

Porvair Sciences, in conjunction with sister company, JG Finneran Associates Inc., has produced a new informative guide to assist laboratory scientists select the optimum seal and closure device for different types of microplate. The guide discusses the different benefits of the most common types of reusable microplate closures (rigid lids, friction seals, and cap mats) and single-use closures (thermal and adhesive seals). An introduction is also provided to Porvair Sciences' extensive range of manual and automated microplate capping and sealing devices.

www.porvair-sciences.com
Porvair Ltd., Wrexham, UK.

SEC mobile phases

Arg-SEC, the universal mobile phase for SEC, enhances protein separations by reducing nonspecific interaction while maintaining protein structure, according to the company. The company reports correct determination of protein aggregates, which tend to stick to columns, is possible and column lifetime may also be improved.

www.nacalai.com
Nacalai Tesque, Inc., Kyoto, Japan.

SEC-MALS detector

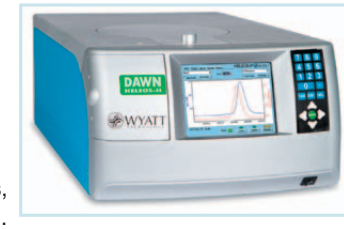

The DAWN Heleos II is an advanced multi-angle static light scattering (MALS) detector for absolute characterization of the molar mass and size of proteins, conjugates, macromolecules, and nanoparticles in solution. According to the company, the DAWN offers high sensitivity, broad ranges of molecular weight, size, and concentration, and a large selection of configurations and optional modules for enhanced capabilities.

https://www.wyatt.com/DAWN
Wyatt Technology, Santa Barbara, California, USA.

LC–MS/MS instrument

PerkinElmer, Inc., has announced the launch of its QSight Triple Quadrupole LC–MS/MS instrument with patented flow-based mass spectrometry that enables laboratories to test highly complex samples and experience increased throughput, according to the company. Combined with PerkinElmer's Altus UPLC instrument, the QSight system reportedly offers a complete solution from sample preparation to results and reporting for food, industrial, and environmental applications. For regulatory food safety purposes, the QSight instrument specializes in detecting a wide range of pesticides that are increasingly found in crops. The system can also test foods for mycotoxins and antibiotics as well as analyze veterinary drugs and nutritional components.

www.perkinelmer.com/Product/qsight-220-multi-opt-dual-source-system-bc003382
PerkinElmer, Inc., Massachusetts, USA.

Pyrolysis for HPLC

The Gerstel PyroVial performs pyrolysis at up to 800 °C. VOCs can be sampled from the headspace, less volatile pyrolysis products are taken up in a solvent for subsequent GC–MS or LC–MS determination. The process is automated using the Gerstel MultiPurpose Sampler (MPS). Placing sample into the reaction chamber is simple. Inert gas phase and reactant(s) can be added.

www.gerstel.com
Gerstel GmbH & Co. KG, Mülheim an de Ruhr, Germany.

HPLC columns

A column designed for current challenges in biotherapeutic drug development is based on a new wide-pore (1000 A) particle. Bioshell IgG columns are suitable for the reversed-phase separation of very high-molecular-weight compounds, such as mAbs, ADCs, aggregates, and fragments with a molecular weight of 150 kDa.

www.SigmaAldrich.com/bioshell
Merck KGaA, Darmstadt, Germany.

Fast GC kit

Designed with GC–MS users in mind, the GC Accelerator kit provides a simple way to speed up sample analysis, according to the company. By reducing oven volume, these inserts allow faster ramp rates to be attained, which reduces oven cycle time and allows for increased sample throughput and more capacity to process rush samples. When faster ramp rates are used, existing methods can be accurately scaled down to smaller, high-efficiency, narrow-bore columns using Restek's EZGC method translator.

www.restek.com/catalog/view/52293/23849
Restek Corporation, Bellefonte, Pennsylvania, USA.

The 32nd International Symposium on Chromatography (ISC 2018)

The **32nd International Symposium on Chromatography (ISC 2018)** will be held on **23–27 September 2018** in **Cannes-Mandelieu, France**.

ISC 2018 is one of the premier meetings to discuss all modes of chromatography and separation sciences with a broad coverage of techniques and applications.

Through a harmonious combination of oral and poster presentations, tutorials, short courses, vendor lectures and seminars, and an international exhibition on instruments and services, **ISC 2018** will provide visitors with the advances, fundamentals, challenges, trends, and applications of separation techniques, chromatography, and mass spectrometry in a wide range of topics.

So far the conference has five confirmed Plenary Lectures to be presented by Alain Beck (Center of Immunology, France), Attila Felinger (University of Pécs, Hungary), Fabrice Gritti (Waters Corporation, USA), Robert Kennedy (University of Michigan, USA), and Peter Schoenmaker (University of Amsterdam, The Netherlands), alongside 33 keynote speakers, six short courses, and six tutorials. The short courses will begin on Sunday 23 September 2018 and will include:

- *Analytical Characterization of Protein Biopharmaceuticals* with Davy Guillarme (Université de Genève, Switzerland) and Koen Sandra (Research Institute for Chromatography, Belgium)
- *Flavours and Fragrances and Analytical Chemistry: An Endless Story* with Xavier Fernandez (University of Nice-Sophia Antipolis, France), Frédéric Begnaud (Firmenich S.A, Switzerland), and Christophe Peres (Chanel SAS, France)
- *Development and Control of Robust HPLC Methods by Modeling* with Szabolcs Fekete (Université de Genève, Switzerland) and Imre Molnár (Molnár-Institute for applied chromatography, Germany)
- *GC×GC: Fundamental Principles, Processes, and Applications* with Philip Marriott (ACROSS, Australia)
- *Microextraction—The "Green" Sample Preparation Choice of Next Generation Analytical Chemists* with Stig Pedersen-Bjergaard (UiO: School of Pharmacy, Norway) and Janusz Pawliszyn (University of Waterloo, Canada)
- *Introduction to Metabolomics Workflow* with Serge Rudaz (Université de Genève, Switzerland) and Coral Barbas (Universidad CEU-San Pablo, Spain)

As the Symposium will take place in Cannes-Mandelieu, Côte d'Azur, a fabulous setting in the French Riviera, the organizers hope that the charm and sweetness of the region in September will give **ISC 2018** a special flavour.

The Congress and Exhibition Centre (Mandelieu Centre Expo Congrès) is easily accessible via International Airport Nice Côte d'Azur by shuttle, taxi, and train. The area also features more than 1000 hotel rooms that are within walking distance from the Congress Centre.

Mandelieu, the Mimosa Capital, is situated on the Esterel Massif. It offers a fantastic setting for a unique destination in the heart of the Côte d'Azur midway between Saint-Tropez and the Italian border.

In addition to the very exciting five-day conference programme, the organizers hope attendees will find time to sample the attractions of the region. The warm temperature in September in Esterel Massif is an ideal location for trekking. For a scientific adventure visit the Sophia Antipolis Science and Technology Park, where many fragrances and perfumes are created. The organizers recommend tasting the southern version of "French cuisine" and experience the hyphenation of the local food with the local wines (in moderation).

The symposium chairpersons are Didier Thiébaut (Université PSL, France), Valérie Pichon (Université PSL, France), and Jean-Luc Veuthey (Université de Genève, Switzerland). For more information, please visit: **www.isc2018.fr**

Photo Credit: ISC2018

26–27 June 2018
The 2nd Copenhagen Symposium on Separation Sciences (CSSS 2018)
DGI-Byen Hotel, Copenhagen, Denmark
E-mail: jorg.kutter@sund.ku.dk
Website: https://cphsss.org

8–11 July 2018
PREP 2018
Hyatt Regency Baltimore Inner Harbor Hotel, Baltimore, Maryland, USA
E-mail: janet@barrconferences.com
Website: www.prepsymposium.org

29 July–2 August 2018
47th International Symposium on High Performance Liquid Phase Separations and Related Techniques
Marriott Wardman Park, Washington, DC, USA
E-mail: janet@barrconferences.com
Website: www.hplc2018.org

22–24 August 2018
2018 Sample Prep Summer Course
Chania, Crete, Greece
E-mail: sampleprep2018@enveng.tuc.gr
Website: www.sampleprep2018.tuc.gr

9–13 September 2018
1st International Conference on Ion Analysis (ICIA-2018)
Technische Universität Berlin, Berlin, Germany
E-mail: wolfgang.frenzel@tu-berlin.de
Website: www.icia-conference.net

17–19 October 2018
12th International Conference on Packed Column SFC (SFC 2018)
Strasbourg, France
E-mail: register@greenchemistrygroup.org
Website: www.greenchemistrygroup.org

21–24 October 2018
7th International Conference on Polyolefin Characterization
Houston, Texas, USA
E-mail: Raquel.ubeda@icpc-conference.org
Website: http://www.icpc-conference.org

27 November 2018
Advances in Clinical and Forensic Analysis 2018
RSC Burlington House, London, UK
Website: https://chromsoc.com/events/

Please send any upcoming event information to lewis.botcherby@ubm.com

Use Promo Code CSC25 for 25% Off Registration!

CANNABIS
SCIENCE
CONFERENCE

Hosted by

jCanna .com

August 29-30, 2018

Portland, Oregon

OREGON Oregon Convention Center

The World's Largest Cannabis Science Conference

returns to downtown Portland for an incredible gathering of analytical scientists, medical professionals, cannabis industry experts and novices interested in learning more about cannabis science!

Sponsorship and exhibition opportunities are still available. Contact Josh Crossney at josh@jcanna.com for more info.

CannabisScienceConference.com

jCannaInc
jCanna_Inc
@jCanna_Inc

SHIMADZU
Excellence in Science

50th ANNIVERSARY Shimadzu Europa

Switch + Go

Nexera UC/s allows measurements by liquid chromatography (LC) as well as supercritical fluid chromatography (SFC) on a single system. An increased range of compounds can be analyzed as LC and SFC offer very different selectivities for analytes of interest. Switching between LC and SFC permits rapid screening for optimum separation conditions, resulting in improved analytical efficiency.

Improved analytical results and efficiency
using two different separation techniques

Smaller footprint, reduced cost of acquisition
while benefiting from a full SFC/UHPLC setup

Automated workflow
to create LC/SFC screening sequence

Upgrade of existing LC to SFC functionality
without the need to buy an additional instrument

Nexera UC/s

www.shimadzu.eu/nexera-ucs